NAM

Groningen 1978-2015 time-lapse gravity surveys results interpretation and scenario testing

NAM

Marcin Glegola, Henk van Oeveren, Leendert Geurtsen, Per Valvatne

Date August 2017

Editors Jan van Elk & Dirk Doornhof

General Introduction

The subsurface model of the Groningen field was built and is used to model the first step in the causal chain from gas production to induced earthquake risk. It models the pressure development in the gas bearing formations in response to the extraction of gas and water.

The reservoir model of the Groningen field was built in 2011 and 2012 and has a very detailed model of the fault zone in the field to support studies into induced earthquakes in the field. The model was used to support Winningsplan 2013 (Ref. 1 to 3) and has since been continuously improved (Ref. 4).

The pressure in the field is an important driver for compaction and therefore subsidence. Compaction in turn affects stress and strain and is therefore of importance for the mechanism inducing earthquakes. Away from the wells penetrating the reservoir, calibration of the model is difficult due to the paucity of available data. Pressure in the aquifers adjacent to the reservoir therefore has larger uncertainty, making it difficult to model water ingress into the reservoir and to forecast reservoir pressure development in the aquifer and reservoir.

One of the options to learn more about the flow of gas and water in the reservoir away from the wells, is a gravity survey. Changes in mass can be deduced from the differences in gravity, measured at different times. NAM therefore acquired a new gravity survey in 2015 (Ref. 6). This report describes how the results of the gravity survey are used to better understand the flow of water and gas in the reservoir and improve the pressure prediction.

References

1. Winningsplan Groningen 2013, Nederlandse Aardolie Maatschappij BV, 29th November 2013.
2. Technical Addendum to the Winningsplan Groningen 2013; Subsidence, Induced Earthquakes and Seismic Hazard Analysis in the Groningen Field, Nederlandse Aardolie Maatschappij BV (Jan van Elk and Dirk Doornhof, eds), November 2013.
3. Supplementary Information to the Technical Addendum of the Winningsplan 2013, Nederlandse Aardolie Maatschappij BV (Jan van Elk and Dirk Doornhof, eds), December 2013.
4. Groningen Field Review 2015 Subsurface Dynamic Modelling Report, Burkitov, Ulan, Van Oeveren, Henk, Valvatne, Per, May 2016.
5. Independent Review of Groningen Subsurface Modelling Update for Winningsplan 2016, SGS Horizon, July 2016.
6. Gravity monitoring of the Groningen gas field 2015, Quad Geometrics, Ola Eiken, April, 2016.

NAM

Title	**Groningen 1978-2015 time-lapse gravity surveys results interpretation and scenario testing**		**Date**	August 2017
			Initiator	NAM
Autor(s)	**Marcin Glegola, Henk van Oeveren, Leendert Geurtsen, Per Valvatne**	**Editors**	Jan van Elk and Dirk Doornhof	
Organisation	NAM, Quad Geometrics	**Organisation**	NAM	
Place in the Study and Data Acquisition Plan	Study Theme: Prediction Reservoir Pressure based on gas withdrawal Comment: The subsurface model of the Groningen field was built and is used to model the first step in the causal chain from gas production to induced earthquake risk. It models the pressure development in the gas bearing formations in response to the extraction of gas and water. The reservoir model of the Groningen field was built in 2011 and 2012 and has a very detailed model of the fault zone in the field to support studies into induced earthquakes in the field. The model was used to support Winningsplan 2013 and has since been continuously improved. The pressure in the field is an important driver for compaction and therefore subsidence. Compaction in turn affects stress and strain and is therefore of importance for the mechanism inducing earthquakes. Away from the wells penetrating the reservoir, calibration of the model is difficult due to the paucity of available data. Pressure in the aquifers adjacent to the reservoir therefore has larger uncertainty, making it difficult to model water ingress into the reservoir and to forecast reservoir pressure development in the aquifer and reservoir. One of the options to learn more about the flow of gas and water in the reservoir away from the wells, is a gravity survey. Changes in mass can be deduced from the differences in gravity, measured at different times. NAM therefore acquired a new gravity survey in 2015. This report describes how the results of the gravity survey are used to better understand the flow of water and gas in the reservoir and improve the pressure prediction.			
Directliy linked research	(1) Model of the gas reservoir (2) Prediction of Compaction and Subsidence (3) Seismological Modelling			
Used data	Gravity Survey Groningen field 2015 – by Quad Geometrics.			
Associated organisation	NAM			
Assurance	NAM internal			

Groningen 1978-2015 time-lapse gravity survey results, interpretation and scenario testing

Date: August 2017

Issued by Glegola, Marcin (PTU/E/Q)

Van Oeveren, Henk (NAM-UPO/T/DL)

Geurtsen, Leendert (NAM-UPO/T/DL)

Valvatne, Per (NAM-UPO/T/DL)

EP number:

Reviewer	Ref. Indicator	Role	Signature
Hein de Groot	NAM-UPO/T/LW	Reservoir engineering	
Remco Romijn	NAM-UPO/T/GD	Geophysics	
Clemens Visser	NAM-UPO/T/GD	Geology	
Ed Biegert	SIEP-PTI/EG	Gravity and Magnetics	

Executive summary

Four gravity surveys were acquired over the Groningen field, in 1978, 1984, 1988 and 1996. These included a maximum of 26 observation points, mostly located at NAM sites. A new, large-scale gravity survey was acquired in September 2015. This survey included 98 gravity stations, 21 of which are 4D observation points at which time-lapse gravity signal is observed. The historical gravity data was re-processed and thoroughly evaluated by a survey contractor leading to some quality improvement and confidence downgrade in the 1984 and 1988 data. Additional sources of time-lapse signal uncertainties were analyzed, including groundwater variations, salt mining, and gas production from neighboring gas fields. The noise from these sources is not significantly affecting the interpretation of historical data. Thanks to the length of the time-span in between the surveys, the analyzed signals are much larger than the potential noise. However, gravity noise from the above sources will become more relevant in the future when time-intervals between subsequent surveys may become shorter and measured gravity changes smaller.

A number of historical gravity observation points were removed after 2001, primarily due to cluster reconstruction work executed as part of the Groningen Long Term project. New stations were established in 2015 at a distance close to original locations and historically measured gravity values were transferred to the new station locations with dedicated gravity gradient measurements. Some stations were affected by significant near surface changes potentially leading to gravity changes and were judged unsuitable for interpretation. The analysis is focused mainly on the 1996-1978 gravity signal because the gravity stations were not affected by any infrastructure changes during this period. The 2015-1978 gravity data is analyzed for those stations where conditions were not altered significantly.

Measured gravity changes range from approximately -50 μGal to +8 μGal for 1996-1978 time interval, and from -84 μGal to +13 μGal for the 2015-1978 time interval. The average time-lapse signal uncertainty is estimated at approximately 10 μGal. The observed gravity changes are consistent with gas water contact (GWC) rise measurements, in wells for which saturation information from pulsed neutron logging (PNL) is available. The mismatch between the measured and modeled gravity shows certain patterns leading to scenario testing with PNL data as additional constraints. The results show that in the North-East of the field around the Bierum cluster of producing wells, more water influx is required to explain the observed gravity changes than currently modelled. The opposite holds for the Stedum area, where gravity changes indicate less water influx than currently modelled. Part of the mismatch in the South of the field can be explained by depletion of the Carboniferous underlying the main Slochteren reservoir. However, scenarios to test this could not account for the entire mismatch observed.

Based on BP_2016_2P production forecasts, gravity calculations were done to assess the suitable timing of a next gravity survey, which is between 2021 and 2023.

The data quality of future surveys is greatly enhanced by the availability of stable gravity stations through time. Therefore, it is recommended to keep track of physical changes at the stations by regular inspections, at approximately 2 year intervals.

Contents

1 Introduction

Time-lapse gravity measurements can detect subsurface mass changes and hence can be used to constrain mass redistribution in the reservoir model, if the signal-to-noise ratio is sufficiently high. Therefore, the technique is especially suitable for monitoring gas fields where depletion and/or water replacing gas leads to large density and mass changes in the subsurface.

Specifically for the Groningen field, time-lapse gravity measurements can provide constraints on gas depletion and water influx to the field, which have an impact on geomechanical behavior, ultimate gas recovery, and reservoir management. Due to uncertainties in the size and exact strength of the aquifers surrounding and underlying the field and the multitude of baffling faults, the water influx into the Groningen field remains uncertain in some areas, especially in areas without well control (where saturation changes can not be measured, Figure 1).

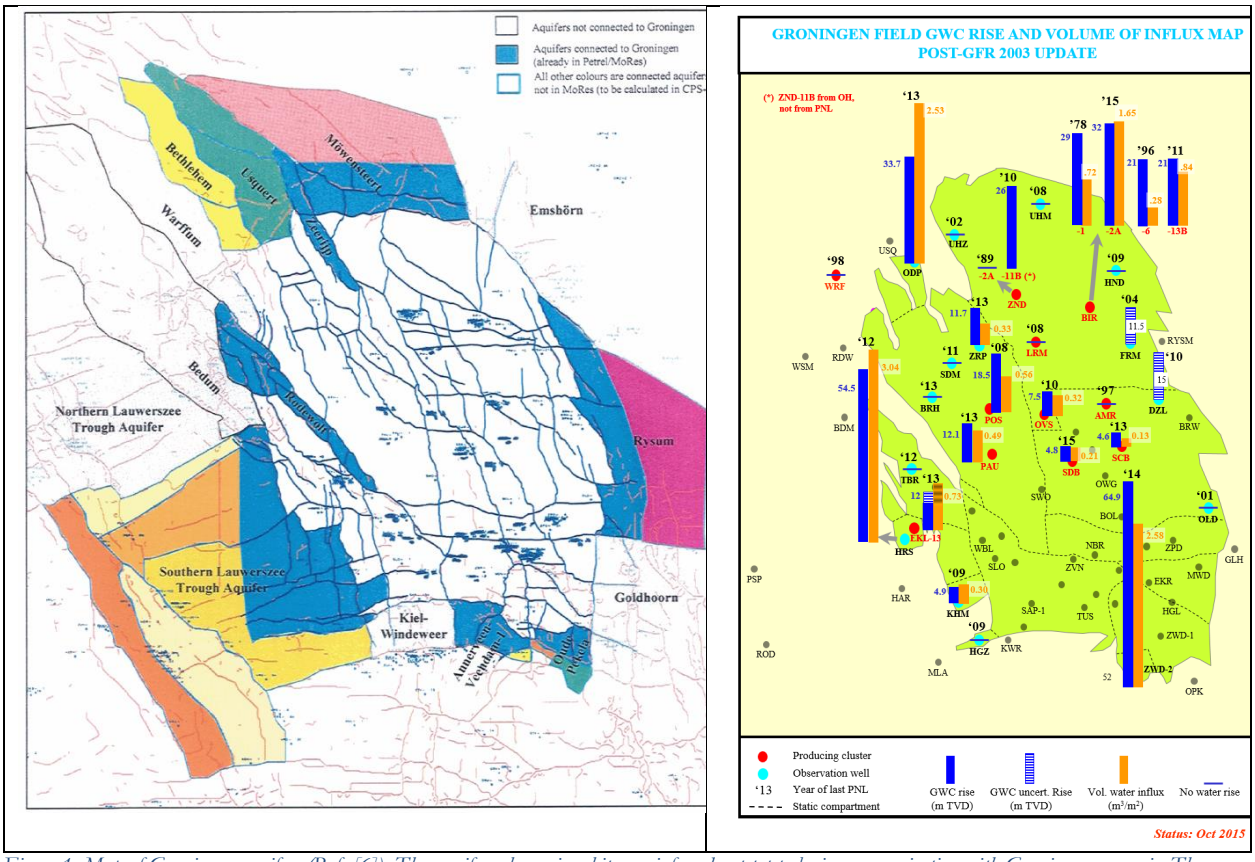

Figure 1: Map of Groningen aquifers (Ref. [6]). The aquifers shown in white are inferred not tot to be in communication with Groningen reservoir. The picture on the right shows measured gas-water contact rise. Status October 2015.

High-precision gravity surveys have been carried at Groningen field repeatedly since the late seventies with measurements acquired in 1978, 1984, 1988, 1996 and the latest in September 2015. The 1978-1996 surveys were acquired by Delft University of Technology (Ref. [1, 4]) and the most recent, 2015 survey, by gravity contractor Quad Geometrics.

- The initial objective of the 1978-1988 measurements was to explore the use of gravity technique as a possible replacement for the costly levelling surveys to monitor land subsidence.
- With increasing time-span in between the measurements, the gravity changes due to gas extraction were expected to be stronger than the noise levels and motivated the 1996 survey. The observed gravity changes from 1978-1996 surveys were compared to the computed gravity effect based on a

simplified reservoir model and production data (Ref. [2]). It was concluded there was an acceptable match, in a statistical sense, between the linear trends derived from the observed gravity changes and those derived from the gas production data. Some spatial differences between the measured and the modelled gravity signal were observed at several locations, however, no definitive conclusions were made at that time.

- The 2015 survey was motivated by a need for complementary field-wide surveillance data, to further constrain uncertainty in the aquifer support. A gravity modelling study, performed in 2014, showed detectable gravity changes between previous surveys and the 2015 survey. Along with the 2015 data processing, the historical survey data have been re-processed and thoroughly evaluated by the gravity contractor Quad Geometrics.

1.1 1978-1996 gravity surveys

The initial gravity network used in the 1978 survey included 21 gravity stations. Additional measurement points were added in subsequent surveys. The network deployed in 1984 consisted of 22 stations, in 1988 survey 23 stations were included and in 1996 the network was further extended to 26 stations (Figure 2). Most of the gravity measurement points were located at NAM sites and some of the stations were part of the national gravity network of the Netherlands NedZwa93 (Figure 3). The full list of 1978-1996 gravity stations is provided in Table 1.

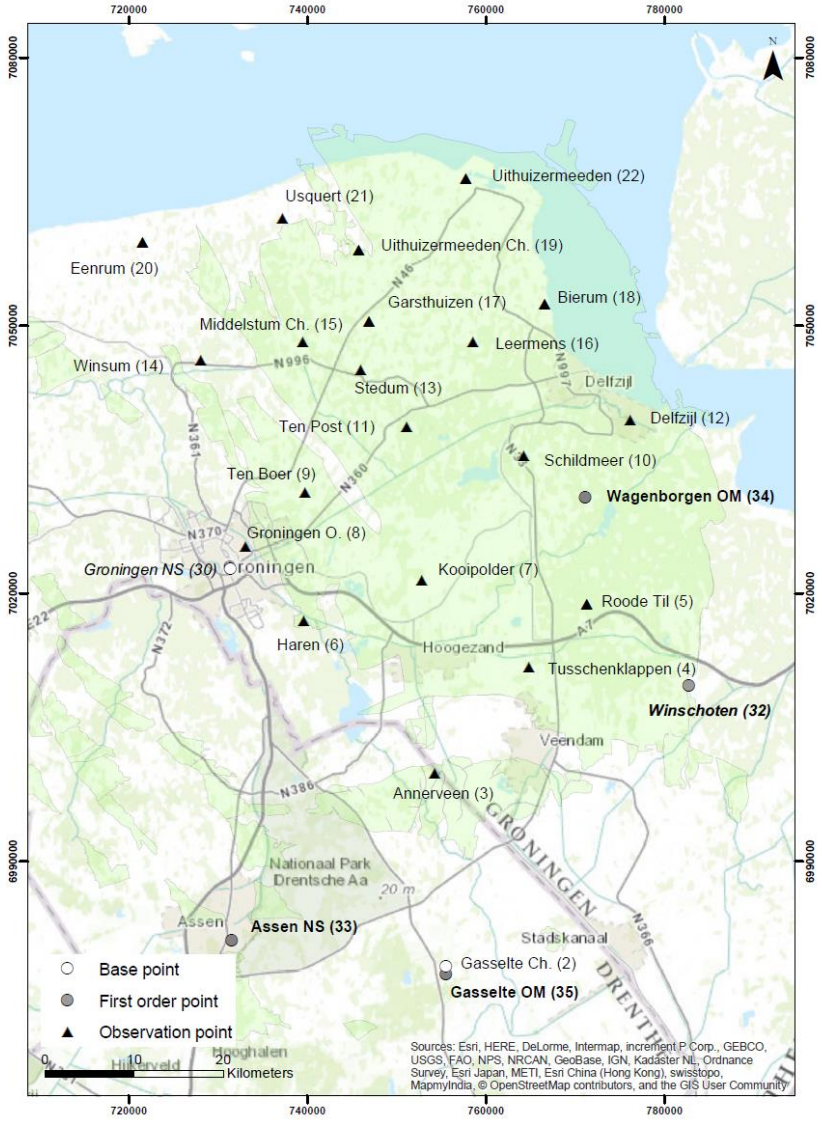

Figure 2: Gravity observation points used in the surveys 1978 to 1996. Italic, bold italic and bold font indicate stations that were added in 1984, 1988 and 1996, respectively. The base points Groningen NS and Gasselte Church are depicted as white dots, the other stations from the Dutch first order network in grey (Ref [7]).

Figure 3: Example of gravity measurement sites used in the 1978-1996 surveys. Left church entrance, right NAM compaction monitoring well – gravity was measured on a cabin floor.

ID (1978-1996)	Station name	1978	1984	1988	1996
3	Annerveen	x	x	x	x
4	Tusschenklappen	x	x	x	x
5	Rode Til	x	x	x	x
6	Haren	x	x	x	x
7	Kooipolder	x	x	x	x
9	Ten Boer	x	x	x	x
10	Schildmeer	x	x	x	x
11	Ten Post	x	x	x	x
12	Delfzijl	x	x	x	x
13	Stedum	x	x	x	x
14	Winsum	x	x	x	x
16	Leermens	x	x	x	x
18	Bierum	x	x	x	x
20	Eenrum	x	x	x	x
21	Usquert	x	x	x	x
22	Uithuizermeeden	x	x	x	x
8	Groningen Oosterpark	x	x	x	x
15	Middelstum Church	x	x	x	x
17	Garsthuizen	x	x	x	x
19	Uithuizermeeden Church	x	x	x	x
2	Gasselte NH Church	x	x	x	x
30	Groningen NS		x	x	x
32	Winschoten NS			x	x
33	Assen NS				x
34	Wagenborgen OM				x
35	Gasselte OM				x

Table 1: Groningen gravity stations measured in the past surveys, indicated with "x". Light blue NAM points, light green public points, light grey base points (public). The base point stations are part of the Dutch first-order gravity network, (Ref. [1]).

1.2 2015 gravity survey

1.2.1 Survey locations

A field inspection of historical gravity sites was carried out in 2015. It showed that the condition of many sites had changed significantly after 2000, primarily due to cluster reconstruction work executed as part of the Groningen Long Term project[1]. To maximize the value of historical gravity data and in order to determine the time-lapse changes with respect to 2015 survey, new gravity stations were established for the affected locations in close vicinity of original points and the gravity values were transferred from their original to the new locations (Figure 4). The station transfer was done a few days before the 2015 survey, with dedicated gravity gradient measurements. The stations which were transferred are added "500" to their original ID, e.g., previously measured station #16 (Leermens) received ID #516.

Figure 4: Example of transferred gravity station measured in the past surveys (Leermens, #516). The original gravity station was inside a control room which was demolished after 2001 (right). The new gravity station (left) was established in a close vicinity of the old point. The gravity values between the two points were transferred with dedicated gravity gradient measurements (photo Ref. [5]).

Compared to the past surveys, the 2015 survey grid was significantly expanded, including 98 gravity stations in total, from which 21 were previously measured points (Figure 5). To provide complementary information, the gravity infill network overlapped with recently installed shallow geophone network measuring seismicity (Figure 6). Thirty-four gravity sites were established at a concrete platform of geophone stations. The remaining gravity infill stations were established at several NAM locations (18 points) or public areas (15 points). The survey was acquired within approximately 2 weeks in September 2015 by Quad Geometrics. To suppress the measurement noise and enhance the data quality each station was visited at least 3 times. Good survey planning, smooth acquisition and data processing resulted in exceptionally low average station uncertainty of 1.1 μGal[2].

[1] During the Groningen Long Term project the production clusters were refurbished as part of the installation of 1st stage compression

[2] 1 μGal = $1 \cdot 10^{-8}$ m/s^2

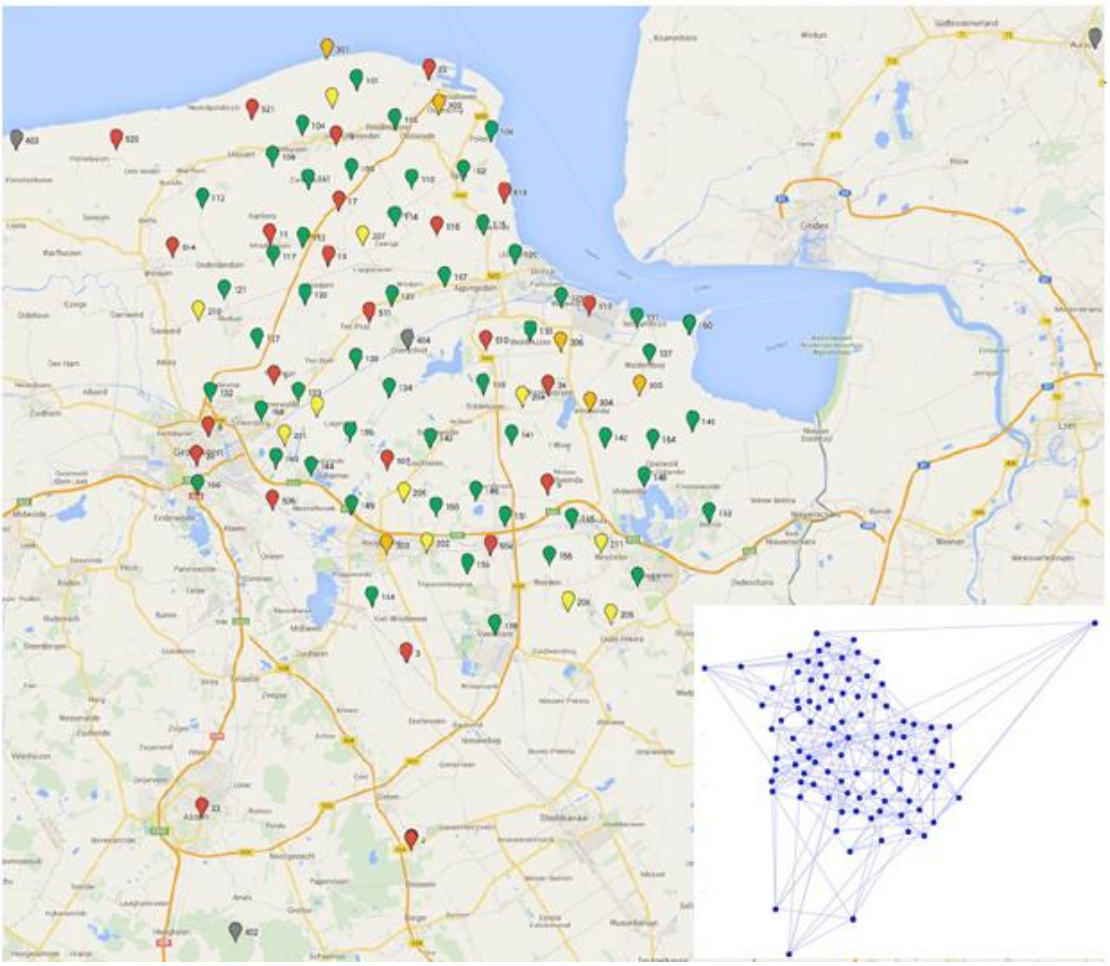

Figure 5: Map of the survey area with gravity stations measured in 2015 shown as droplets: red- previously measured sites, green, yellow, orange) – new infill points; grey – reference stations. The plot on the right shows all gravity loops executed during the survey (Ref. [5]).

1.2.2 Data processing

All raw 1978, 1984, 1988, and 1996 gravity survey data were re-processed and thoroughly evaluated in 2015 by survey contractor Quad Geometrics [Ref 5]. This included e.g., drift fitting, scale factor QC and more accurate tidal corrections. The quality of the historical gravity data slightly improved: the average station uncertainty was reduced from 4-7 μGal down to 3-5 μGal. Reprocessing the historical gravity data did not only help to improve the data quality, but also to better understand the data uncertainties. Significant and systematic discrepancy between the measured and modeled gravity changes for the 1984 and 1988 surveys were observed, in the order of some 12-20μGal (Ref. [5]). Given that this magnitude of mismatch is far beyond the reservoir model uncertainty, which is constrained to production data, it was concluded that the mismatch must (largely) originate from data uncertainty. Based on this, the confidence in 1984 and 1988 survey data has been downgraded and these data sets were not used in the analysis presented in this report.

Figure 6: Example of gravity measurements at one of the geophone network locations (photo Ref. [5]).

2 Measured time-lapse gravity changes

The total measured changes in gravity at Groningen can be attributed to a number of factors:

- Gravity changes due to reservoir production
- Survey site surface modifications
- Groundwater table variations
- Salt mining
- Depletion of neighboring gas fields

This chapter discusses these individual components, and their contribution to the total uncertainty in the measured signal.

2.1 Gravity changes due to reservoir production

Time-lapse gravity signal is a measure of mass changes in the subsurface. The signal directly correlates with net mass change, i.e., it is negative when the net mass change in the subsurface is negative and it is positive when the overall mass variations are greater than zero. In the context of gas field monitoring the negative gravity change indicates that the mass change due to gas extraction is larger than the mass change caused by the water influx. The opposite scenario, indicated by positive gravity changes, is caused by water replacing gas which is of particular interest as it can indicate areas with water influx. This can be summarized in a simplified form with the following equation:

$$\Delta m_{total} = \Delta m_{gas} + \Delta m_{water,}$$

Δm stands for mass change.

In practice, the total gravity change is a combination of water influx and gas extraction, thus the water influx signal can be partly masked by the gas production signal. However, more detailed analysis, with the use of a dynamic reservoir model constrained to pressure and production data, can improve the understanding of water influx into the field. This will be discussed in one of the following sections.

The total time-lapse gravity changes measured at (or at close vicinity of) historical gravity points for 1996-1978 and 2015-1978 are shown in Figure 7. For both time periods, the negative gravity changes dominate and are concentrated in the central part of the field. The signal ranges from approximately -50μGal to +8μGal for 1996-1978 and from -84μGal to +13μGal for 2015-1978 period.

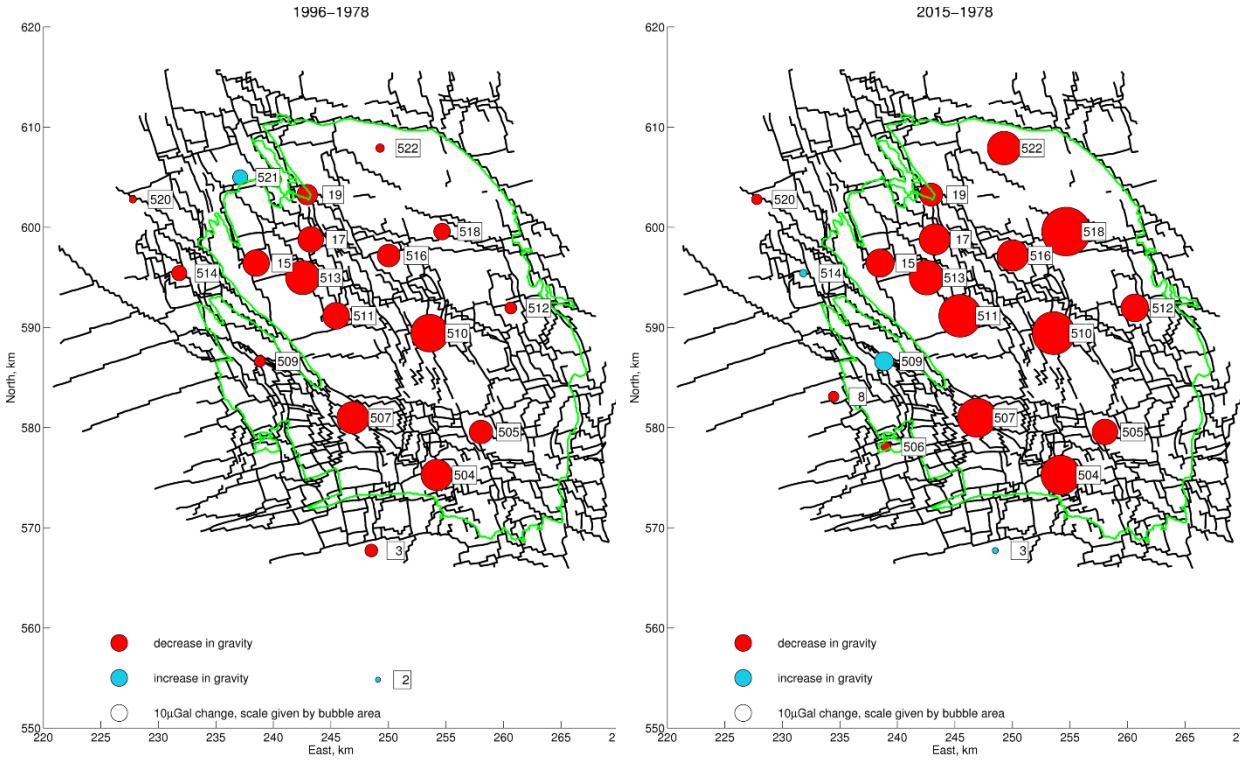

Figure 7: Measured time-lapse gravity changes: left 1996-1978, right 2015-1978. The negative gravity changes are shown in red and the positive in blue. The signal magnitude is proportional to the bubble size. Station numbers are shown in small boxes next to it. Green contour shows the field outline. Major fault boundaries are shown with black polygons.

2.2 Subsidence

Gravity signal changes are caused by subsurface mass changes, but also by changes in height of the measurement points (approximately 3 μGal/cm). Therefore, time-lapse gravity must be corrected for surface subsidence . Subsidence data for 1978-2015 surveys is shown in Table 2 and

Figure 8 and Figure 9. The average height measurement uncertainty estimate of 1.5 cm was used in the gravity data processing translating into a 6.5μGal time-lapse gravity uncertainty.

No	Station name	Height 1978 (NAP)	1984-1978	1988-1978	1996-1978	2015-1996
2	Gasselte church	17.84	0	0.001	0	-0.003
3	Annerveen	2.05	-0.02	-0.034	-0.05	-0.030
4	Tussenklappen	-0.43	-0.01	-0.036	-0.05	-0.077
5	Roode Til	-0.63	-0.03	-0.034	-0.04	-0.068
6	Haren	0.50	0.01	-0.017	-0.03	-0.051
7	Kooipolder	-0.28	-0.03	-0.054	-0.05	-0.085
8	Goningen Sint Fraciscuskerk	0.92	-0.02	-0.030	-0.04	-0.062
9	Ten Boer	-0.34	-0.04	-0.060	-0.08	-0.077
10	Schildmeer	-0.85	-0.05	-0.044	-0.07	-0.093
11	Ten Post	-0.15	-0.04	-0.067	-0.10	-0.135
12	Delfzijl	0.06	-0.03	-0.059	-0.08	-0.069
13	Stedum	1.18	-0.08	-0.109	-0.15	-0.115
14	Winsum	0.86	-0.02	0.001	0.01	-0.043
15	Middlestum church	3.07	-0.04	-0.068	-0.10	-0.076
16	Leermens	1.13	-0.06	-0.078	-0.10	-0.117
17	Garsthuizen Garage	2.20	-0.08	-0.113	-0.14	-0.101
18	Bierum	1.21	-0.03	-0.056	-0.07	-0.099
19	Uithuizermeeden church	2.81	-0.07	-0.073	-0.10	-0.079
20	Eenrum	1.64	0	-0.021	-0.03	-0.025
21	Usquert	1.73	-0.02	-0.035	-0.05	-0.045
22	Uithuizermeeden	1.85	-0.04	-0.058	-0.09	-0.080
30	Groningen NS	3.421	1984 = reference	-0.010	-0.02	-0.039
33	Assen NS	11.146	-	-	1996 = reference	-0.004
34	Wagenborgen OM	1.264	-	-	1996 = reference	-0.082
35	Gasselte OM	15.009	-	-	1996 = reference	-0.003

Table 2: Height and subsidence for the pre-2015 stations, in meters (Ref. [5]).

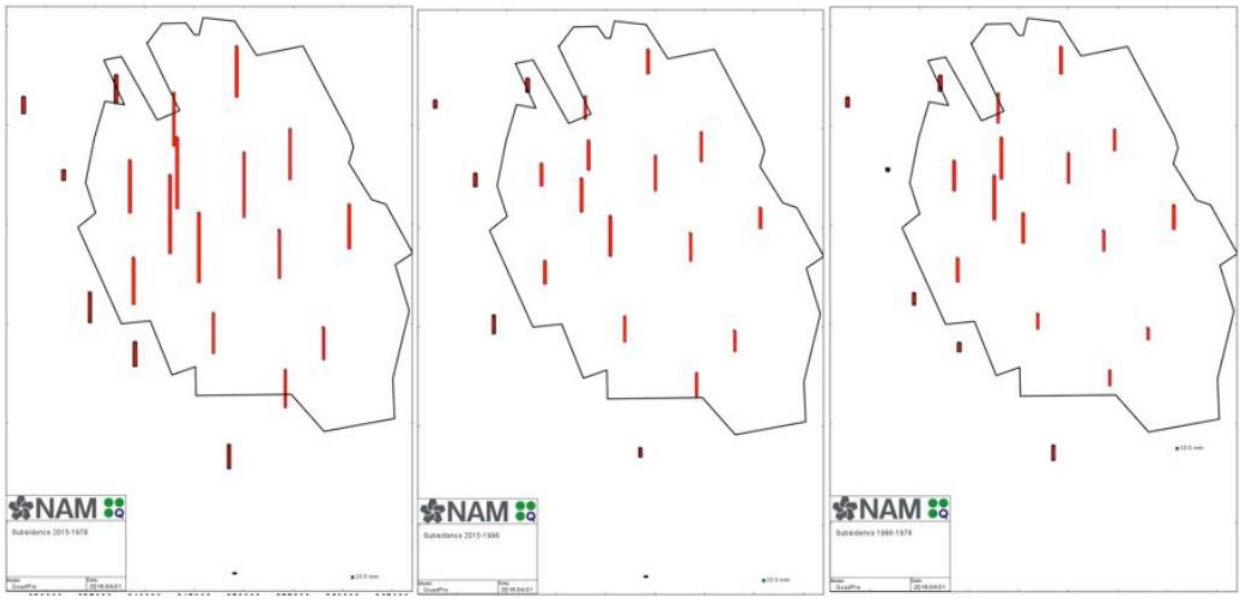

Figure 8: Subsidence data for: 2015-1978 (left), 2015-1996 (middle) and 1996-1978 (right), Ref. [5].

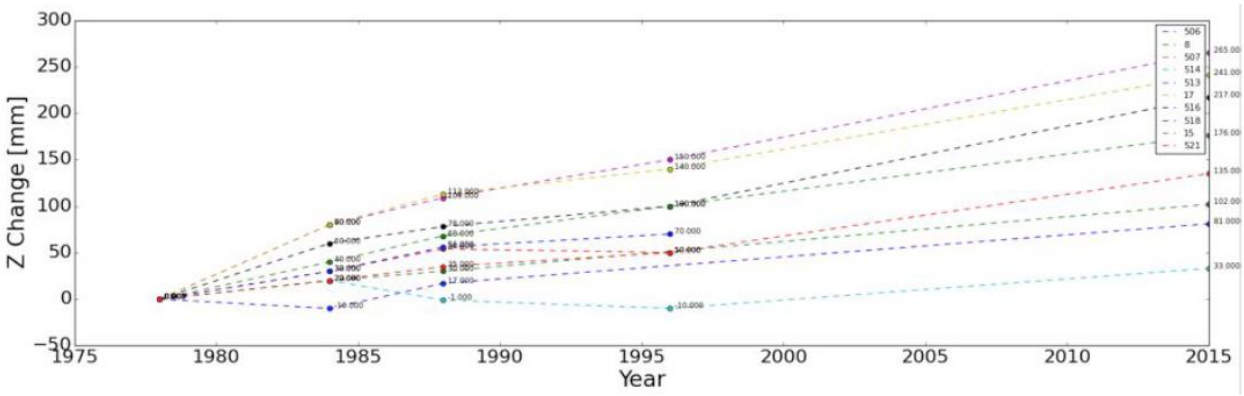

Figure 9: Subsidence development through time compared to 1978 at some stations (Ref. [5]).

2.3 Nearby surface changes

Various gravity stations were affected by nearby surface modifications and had to be transferred (section 1.2.1). An extreme example is Uithuizermeeden station (#522), where large modifications have taken place. A number of oil tanks have been built in close vicinity to this station, and it is likely that a significant amount of soil was removed to build solid tank foundations. This all led to local mass changes around the stations, which are challenging to quantify. A clear change in trend of measured time-lapse gravity in 2015 can be seen, reducing the confidence gravity changes at that particular station in the period 2015-1978.

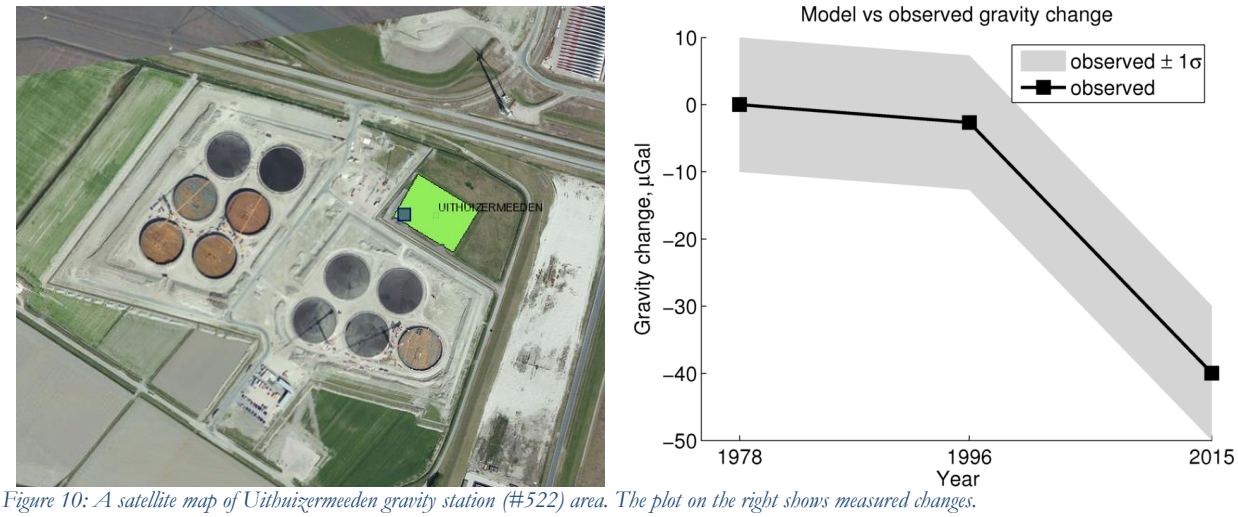

Figure 10: A satellite map of Uithuizermeeden gravity station (#522) area. The plot on the right shows measured changes.

A number of other historical stations have also seen changes, but these changes were far less dramatic. An example is station Schildmeer (#510), where no significant infrastructure changes took place at the direct station neighborhood. In this case the measured gravity signal seems to follow the pattern expected from reservoir depletion, i.e., more gravity reduction in earlier years where rates of production/pressure drop were higher, followed by more subtle gravity decline (Figure 11).

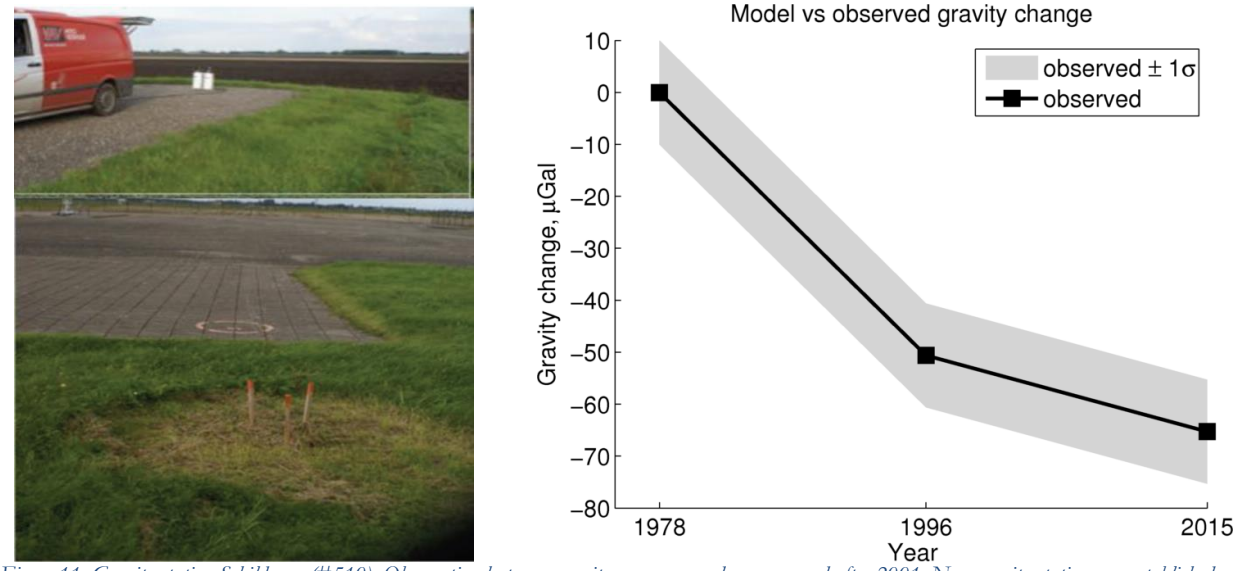

Figure 11: Gravity station Schildmeer (#510). Observation hut were gravity was measured was removed after 2001. New gravity station was established on asphalt outside facility fence. The plot on the right shows measured gravity changes. Picture Ref. [5].

The primary focus in the analysis to follow will be the 1996-1978 gravity signal, as then the gravity stations were not affected by any infrastructure changes. The 2015-1978 gravity change will mainly be analyzed at those stations for which conditions were not altered, like public churches, or for which alterations were not significant, like a few NAM sites, such as Schildmeer.

2.4 Hydrological noise

Environmental effects, specifically variations in groundwater level, contribute to the total uncertainty in the time-lapse estimate of subsurface mass change. In 2015, an MSc project was set up with Delft University of Technology to characterize the hydrological system in the Groningen area and to understand potential implications of groundwater variation on past and future gravimetric monitoring of the field (Ref. [7]). A significant amount of historical records of groundwater data and descriptions of shallow subsurface properties were collected from the DINOloket[3] database and analyzed. The results showed that the soil properties vary significantly in the area (Figure 12), from fine sand in the North, silt and peat in the central part of the area and sand again in the South. Soil type has an impact on the magnitude of groundwater variations, which are typically stronger in a sand environment than in a clay environment (Figure 13). Based on the analysis of historical groundwater level measurements the study showed that the groundwater variations are rather moderate in the area of interest and stay typically below ±1 m. A practical upper bound of 1 m groundwater level change, assuming a soil porosity of 25-35%, could translate to ~10-15 µGal of hydrological noise. Hence, it is not dominating over the signal of interest, which is within 50-80 µGal, but still shall be considered, especially in the context of future more frequent gravity monitoring.

The example shown in Figure 14 compares an estimate of groundwater noise magnitude, as determined in Ref. [7], to the measured 1996-1978 gravity changes. The average noise magnitude is in the order of ~3 µGal in this case and is significantly smaller than the measured gravity changes.

[3] https://www.dinoloket.nl/

Additional insights on spatio-temporal dynamics of the hydrological system in the Groningen area were provided by gravity contractor Quad Geometrics in 2016 (Ref. [5]). The findings highlighted a large number of dikes and canals cross-cutting the survey area where the water level is controlled by automatic water pumps. Much of the area is typically within 100 m from an open dike, meaning that the groundwater level must be correlated with the water level maintained in the dikes and the canals. Active water management in the area falls under the government body of water management and dike surveillance: "Waterschap Noorderzijlvest" and "Waterschap Hunze en Aa's" (Figure 15). Water levels are recorded at several places in the area and controlled at a desired level with water pumps discharging the excess water via canals to the North Sea (Figure 16). The water level is kept relatively stable in most of the area with localized seasonal variations in the order of 0.5-1 m (Figure 17).

Due to insufficient data coverage, i.e., in many cases lack of historical groundwater measurements in a close vicinity of gravity observation points (Figure 12), no hydrological corrections were applied to the 1978-2015 time-lapse gravity data. The analysis of hydrological data presented in Ref. [7] showed that potential groundwater noise is not a dominating factor in the 1978-1996 gravity signal, thus is assumed not to hamper the interpretation significantly. However, it may be relevant for the future field monitoring in case time-intervals between the consecutive gravity surveys become shorter and/or measured gravity changes are smaller.

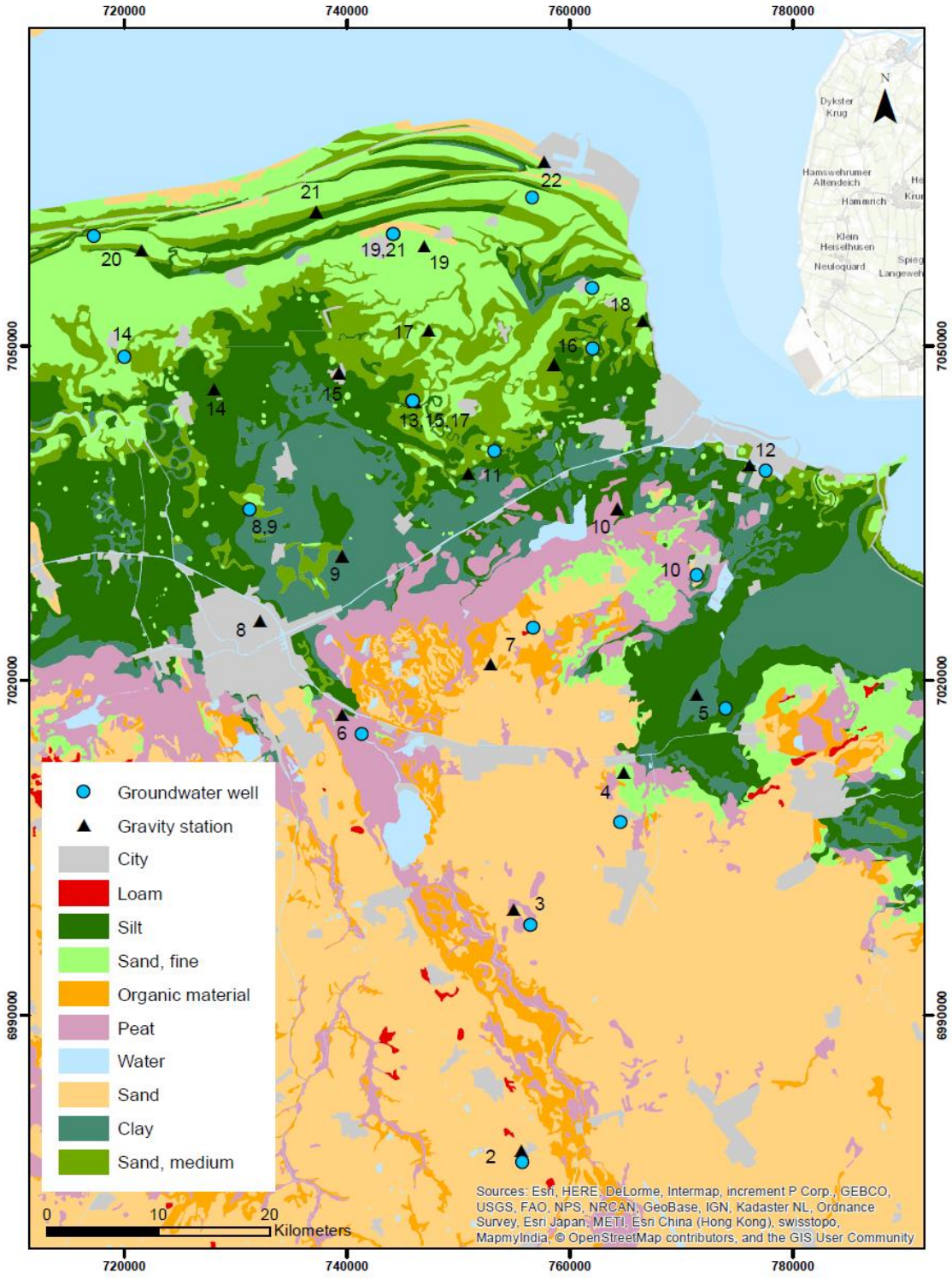

Figure 12: Dominating soil type in the first 1.2 m of subsurface. The locations of historical gravity stations are indicated by black triangles and the nearest groundwater wells with available data with blue dots. From Ref/ [7]. . The lithological map was made by Alterra(2006) http://www.wageningenur.nl/ .

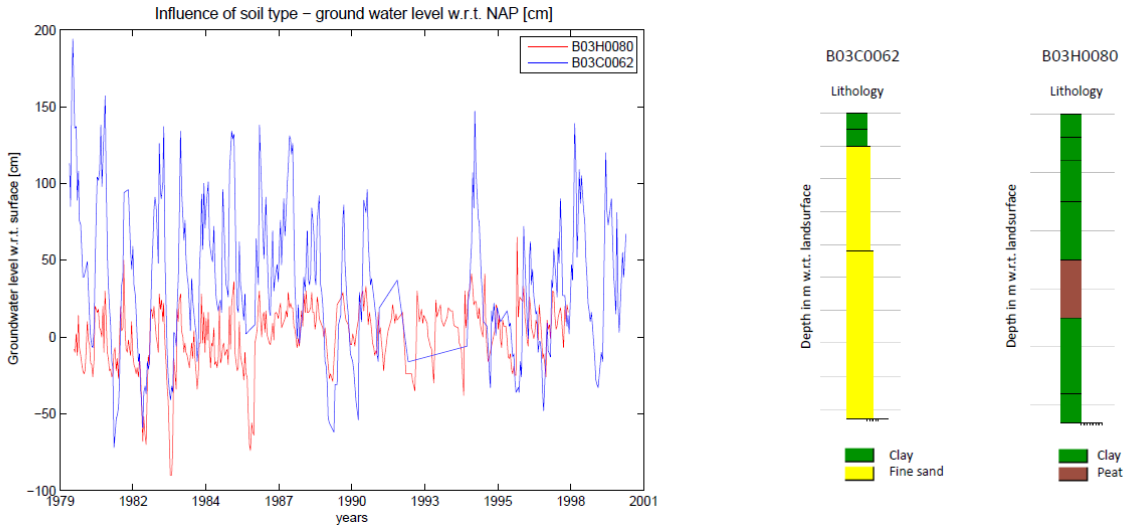

Figure 13: Groundwater variations for well B03H0080 (red) and B03C0062(blue), which are situated in a clay and sand environment, respectively. Groundwater measured in well situated in clay shows much smaller variations in time in the order of 20cm as compared to the other well showing average variations in the order of 40-50cm. The filter depth for the two wells is similar (from Ref. [7]).

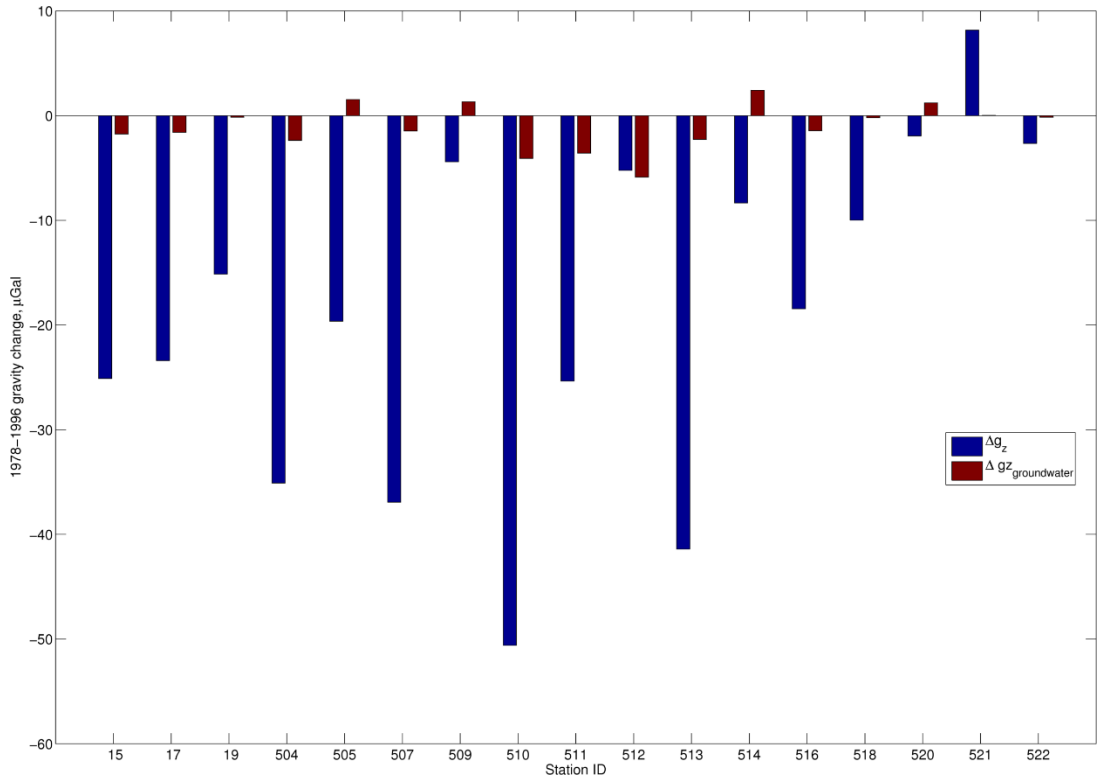

Figure 14: Estimates of gravity noise (dark red) due to groundwater variations (from Ref/ [7]) compared to measured 1996-1978 gravity changes.

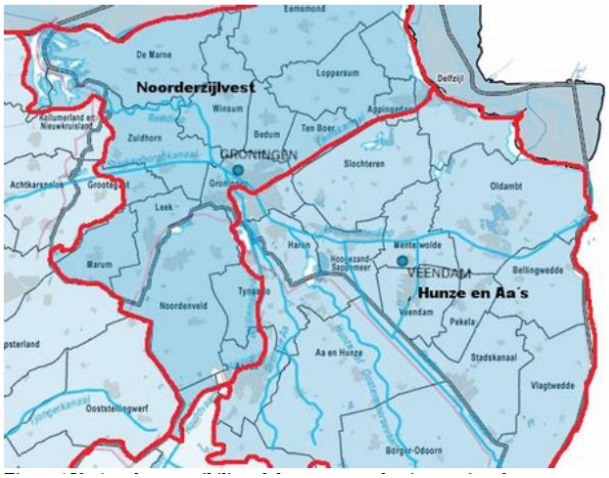

Figure 15 :Areal responsibility of water management organizations Noorderzijlvest and Hunze en Aa's (from Ref. [5]).

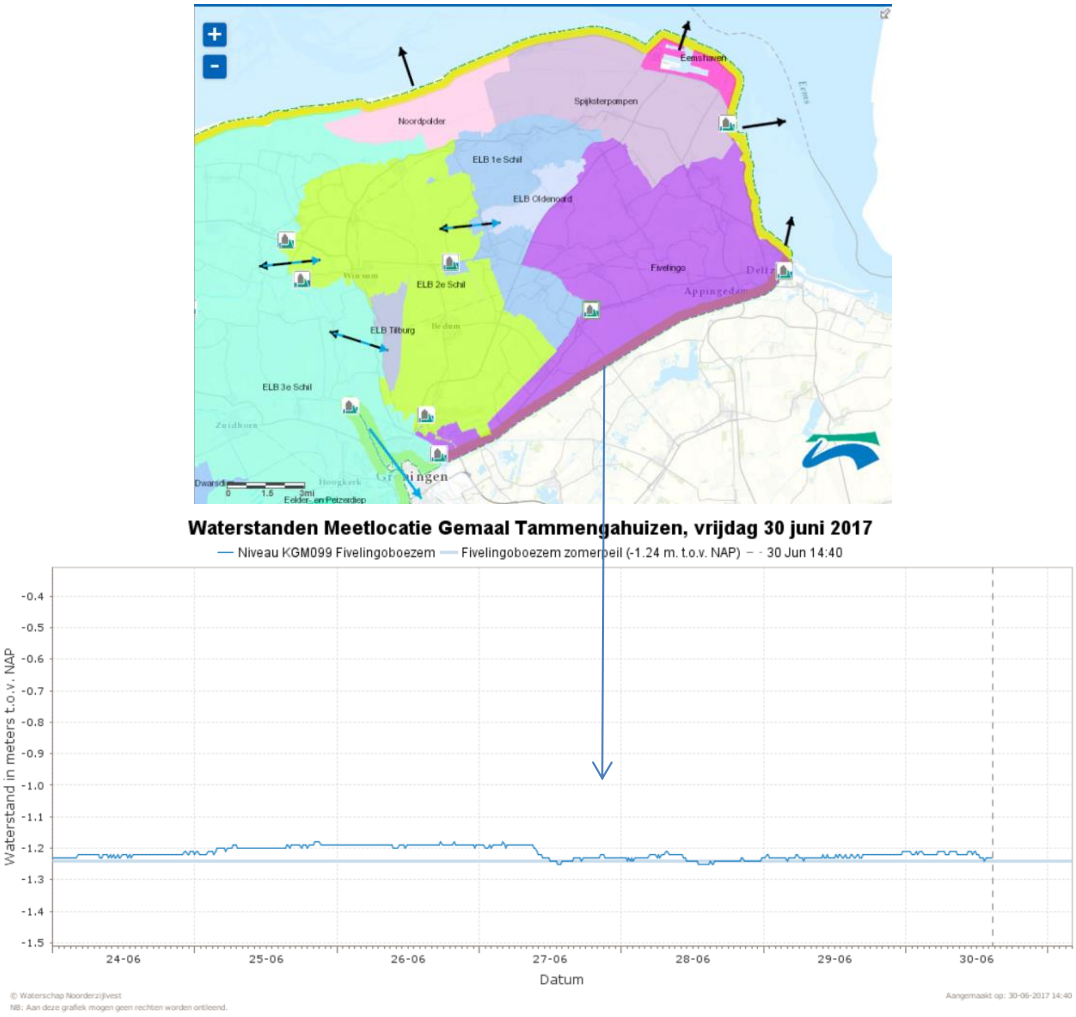

Figure 16: Noorderzijlvest water management map. Water levels are recorded with stations shown with symbols on the maps and the water is discharged to the sea in areas highlighted with black arrows. Example of water level from one of the locations is shown in the bottom plot. Source https://geo.noorderzijlvest.nl/viewer/index.html?webmap=493a84a5e14a49ada4b2ce9176c020d1

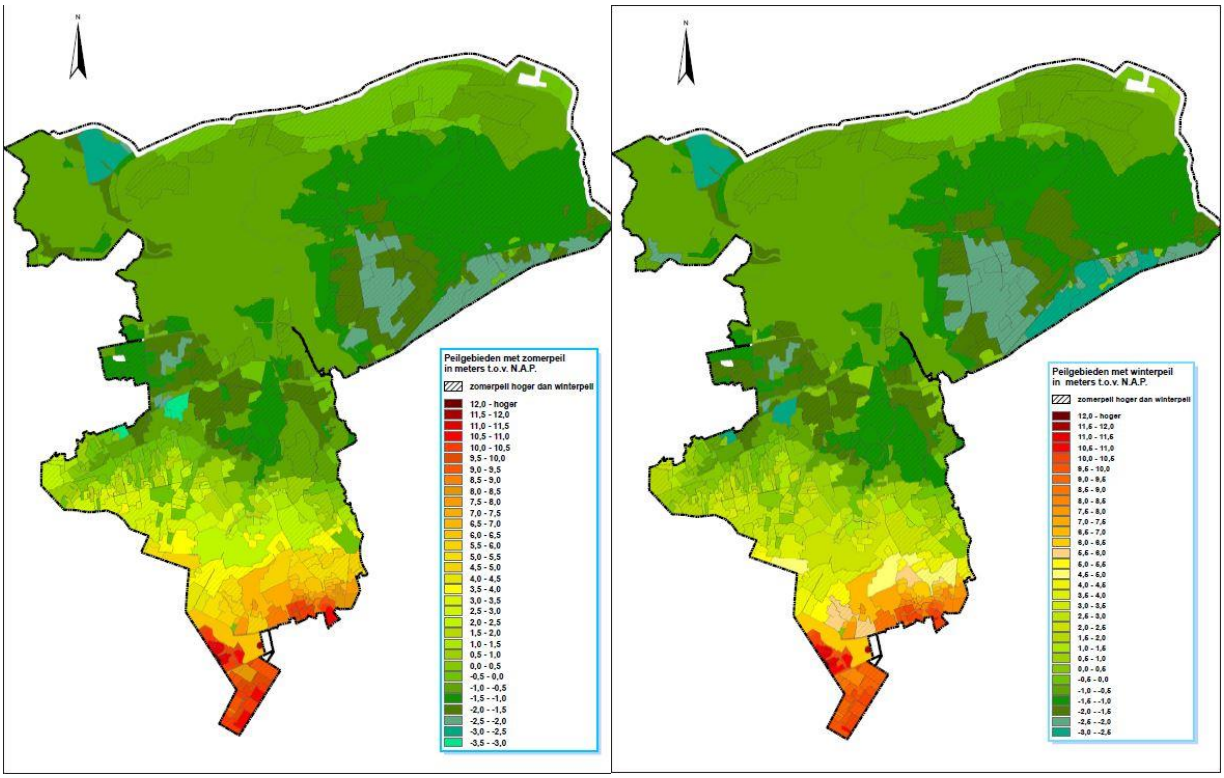

Figure 17: Summer (left) and winter (right) water levels as decided by Noorderzijlvest water management body. After Ref. [5]. Pictures from https://www.noorderzijlvest.nl/actueel/waterstanden/zomerpeil-winterpeil/

2.5 Time-lapse gravity noise due to salt mining

Salt mining yields subsurface mass changes and a subsequent time-lapse gravity signal. In the context of the Groningen reservoir gravity survey this can be considered as a time-lapse noise.

The salt is produced by solution mining where fluids are injected through the wells to dissolve the salt (Figure 19). After some period of time the mixture of fluids and salt is produced back to the surface where the salt is extracted. The fluids are re-injected and the whole process is repeated. Based on the salt mines production data, available at www.nlog.nl, an attempt was made to quantify the magnitude of corresponding time-lapse gravity noise.

There are three active salt mining permits in the Groningen survey area (Figure 18): Veendam, Adolf van Nassau and the extension of Adolf van Nassau. Within these permits the oldest mine is at Winschoten, which has been producing salt since 1954, followed by Zuidwending which started production in 1967 and Veendam which has been in production since 1972. Only the salt production data from 2005-2015 was available from www.nlog.nl for this study. The total amount of salt produced for the 2005-2015 period is approximately 25.5 million tons. The total salt production covering 1978-2015 was approximated by assuming equal production levels before and after 2005. This is likely to be an upper bound of total salt produced

between 1978-2015 as salt output levels were increasing slightly with time as new production wells were added. Multiplying 2005-2015 total production with 3.7 to reflect the difference in the number of production years (10 for 2005-2015 vs 37 for 1978-2015) gives approximately 94 million tons of salt produced in the period 1978-2015.

The production well coordinates and well depths were retrieved from www.nlog.nl. Extracting salt with solution mining leads to the formation of caverns around the well. The caverns are up to 125m in diameter and vary in height from 550 to 850m (Figure 20). To model the gravitational effect of produced salt, the point mass approximation is used (Appendix 1). This is certainly a simplification but is considered sufficient to estimate an order of magnitude of gravity change caused by salt extraction. Based on well depth penetration data and cavern geometries the average depths of point sources are assumed. They are 1200m for Winshoten, 1500m for Veendam, and 900m for Zuidwending.

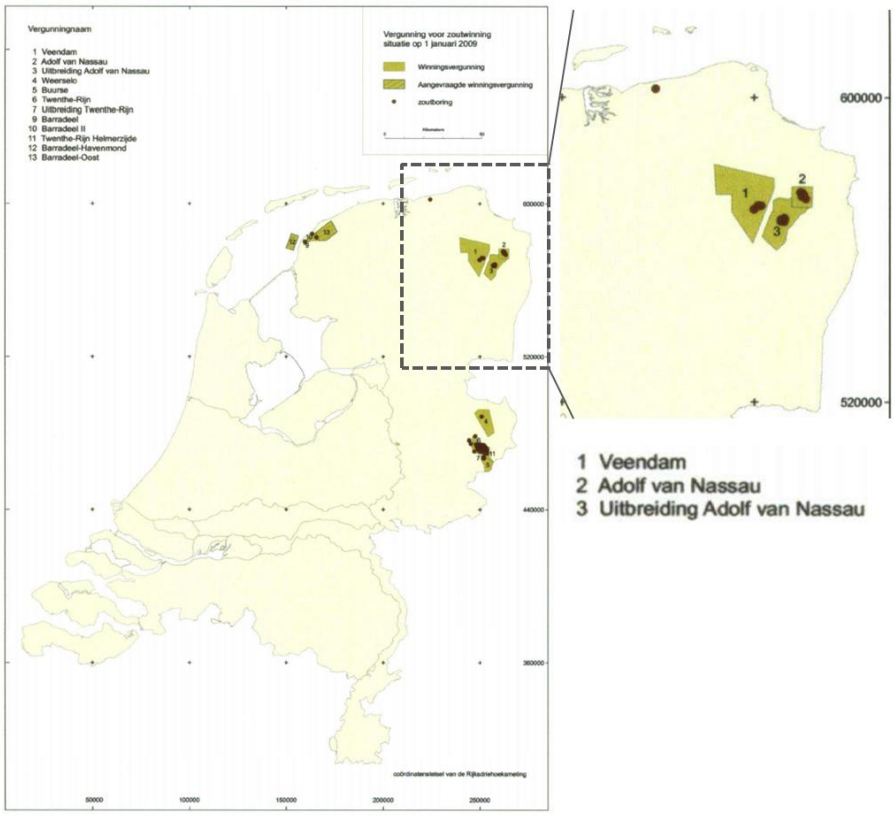

Figure 18: An overview of map salt mine locations in the Netherlands. Picture modified from Ref. [8].

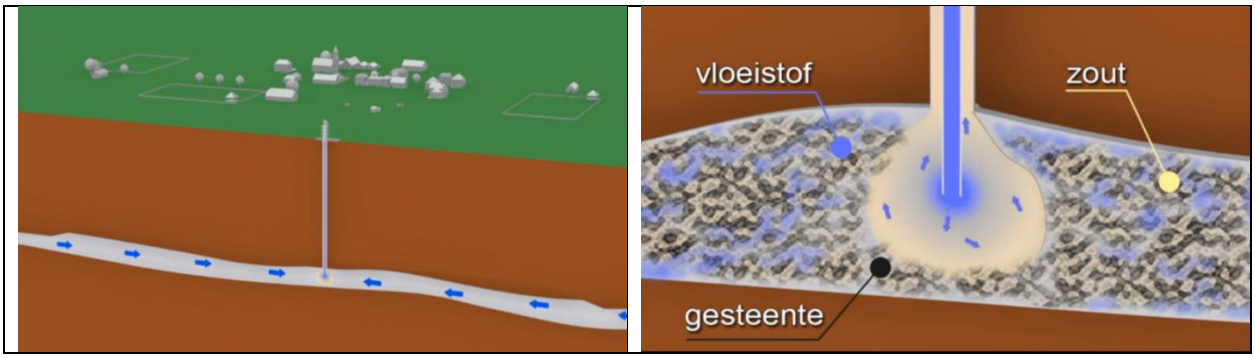

Figure 19: Schematic illustration of salt production method applied at Veendam. Source www.nedmag.nl

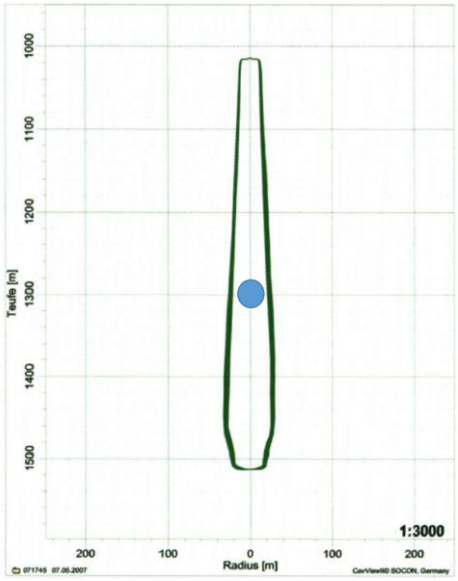

Figure 20: Schematic illustration of cross section through the salt cavern at one of the Winschoten wells. The blue dot shows the position of the point source representing the mass reduction within the cavern. Picture modified from Ref. [8].

The modelled gravity effect due to salt production overlaid with measured 2015-1978 time-lapse gravity changes is shown Figure 21. The gravity change due to salt mining at time-lapse stations used in the analysis is very limited. The signal is in the order of -1.5 μGal for station 504 and approximately -0.4 μGal for station 505, and hence it is not of a concern for 1978-2015 time-lapse data interpretation. However, the signal can reach several tens of μGal at close proximity to the production wells which are not far from some of the new gravity stations measured for the first time in 2015. This shows that gathering salt production data and running more detailed gravity modeling will be very relevant with future time-lapse gravity surveys at the Groningen field.

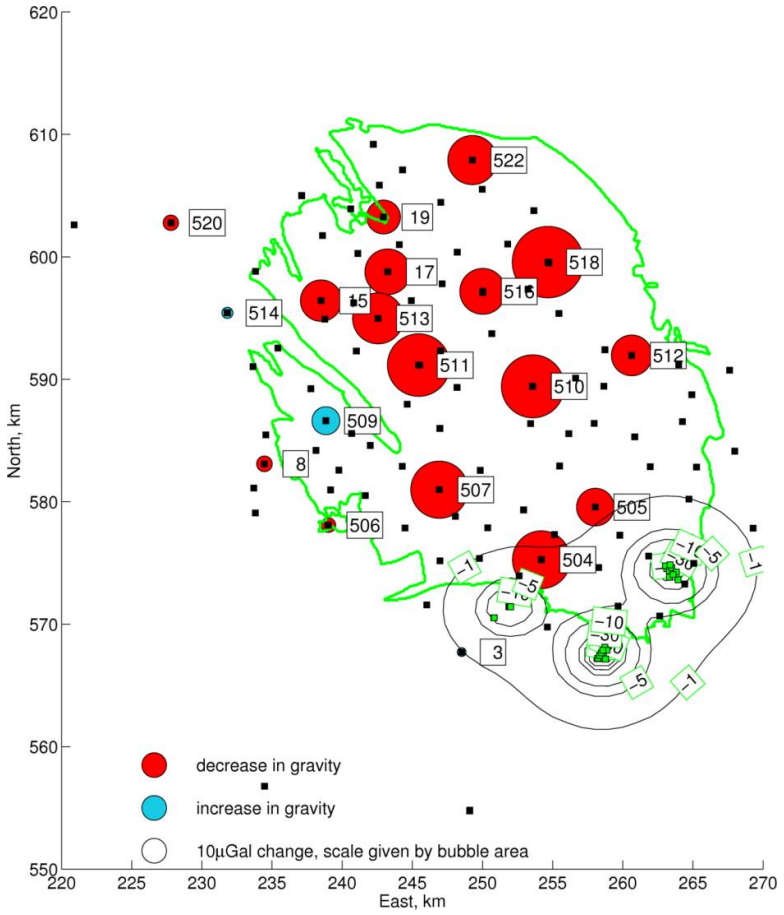

Figure 21: Modelled gravity effect due to salt extraction for 1978-2015 period (black contours). In the background measured time-lapse gravity changes for the same period are shown (circles). With green squares salt production wells are shown and the black squares show location of all gravity stations measured in 2015.

2.6 Time-lapse gravity noise caused by depletion of neighboring gas fields

Another potential source of time-lapse gravity noise affecting interpretation of Groningen gravity data is mass reduction due to production of neighboring gas fields. The largest neighboring field is the Annerveen gas reservoir. Based on the field yearly production data, gravity modelling is done to quantify the gravity effect due to Annerveen depletion. The average reservoir depth is 2900 m, the average thickness is 100 m and the porosity varies from 8-15%. The total mass reduction caused by gas takeout is approximately 44 million tons for 1978-2015 period. Any water influx into the field would decrease the net mass change and hence reduce the total gravity effect. No significant aquifer support is present at Annerveen, but the amount of water influx to the reservoir remains uncertain. The gravity modelling is based on mass change due to gas takeout only. This scenario can be seen as the practical upper bound of gravity effect influencing infield Groningen time-lapse gravity stations. The gravity modeling is based on point mass approximation. Because the extent of the Annerveen field is significant, some 6000 uniformly distributed point mass sources were used to model the gravity effect more accurately. This gives a maximum gravity change of ~9 μGal at the center of the field and -0.8 μGal at monitoring station Tussenklappen (504) which is the closest to Annerveen reservoir (Figure 23). The gravity effect further decays with distance and it is ~-0.24 μGal at station #507 and close to zero at station #510.

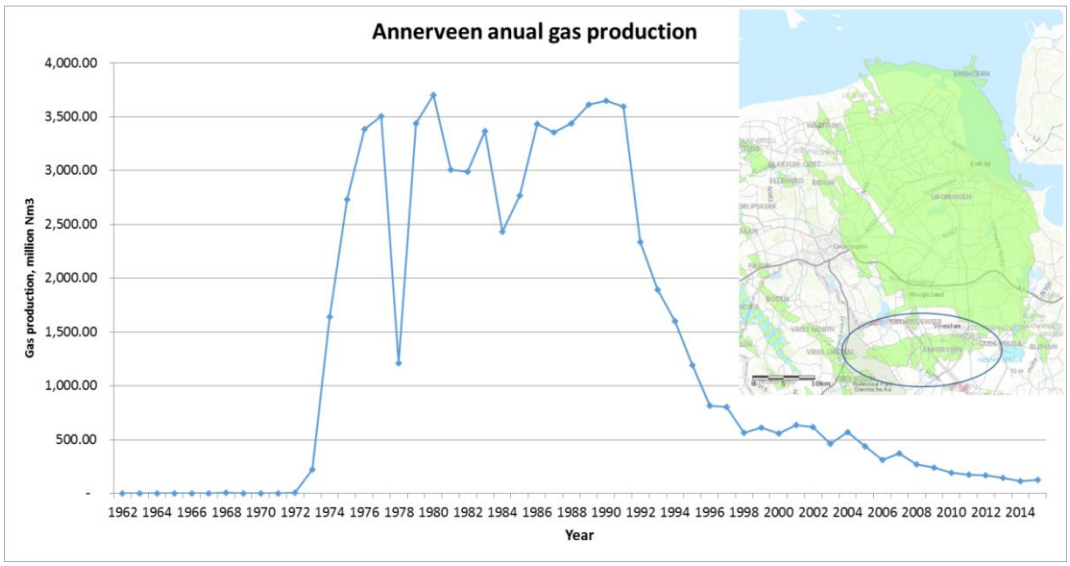

Figure 22: Annerveen field yearly gas production.

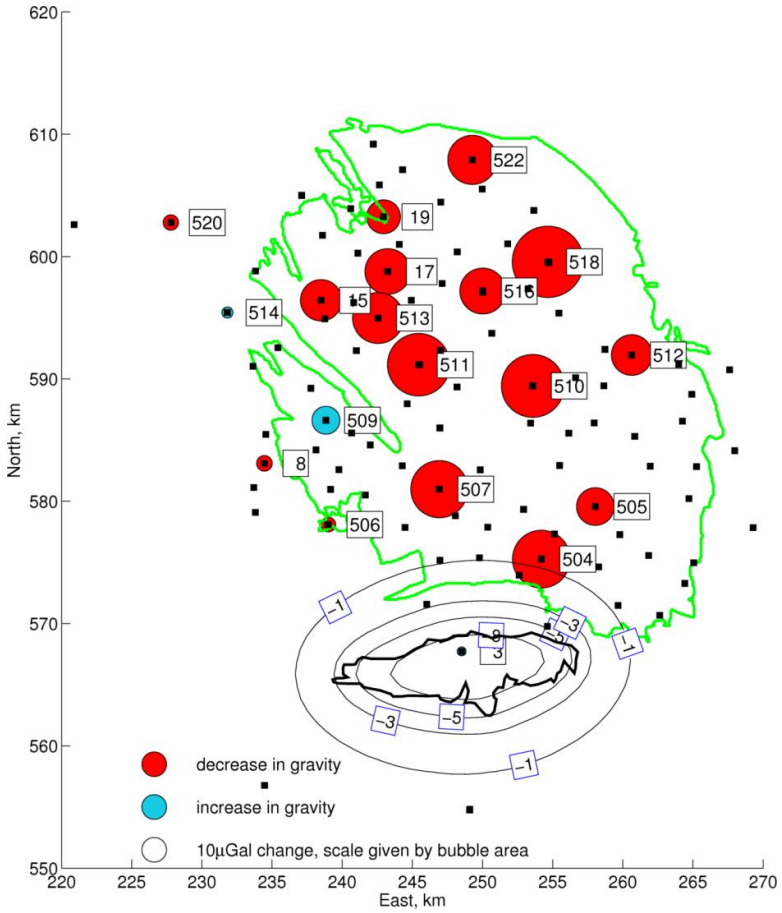

Figure 23: Modelled gravity effect due gas production at Annerveen field (black outline) for 1978-2015 period (black contours). In the background measured time-lapse gravity changes for the same period are shown (circles). Black squares show stations measured in 2015.

2.7 Time-lapse signal uncertainties

Table 3 and Table 4 show a summary of measured gravity changes and the corresponding time-lapse error estimates. The "Change in g" column shows the measured gravity change, "Change in g, corrected" shows the measured gravity changes corrected for land subsidence. The uncertainty on subsidence measurements is included in the total gravity error estimate (last column) which is larger than that for the "raw" gravity changes (Ref. [5]). The average time-lapse gravity error estimate is approximately 10μGal.

Station	X (m)	Y (m)	Change in g (μGal)	Std. dev. g (μGal)	Change in z (cm)	Std. dev. z (cm)	Change in g, corrected (μGal)	Total error estimate for g corr., (μGal)
2	249094	554823	1.0	5.7	0.0	2.1	1.0	12.2
3	248512	567725	9.4	7.3	-5.0	2.1	-6.0	11.3
15	238498	596425	5.7	7.2	-10.0	2.1	-25.1	10.0
17	243244	598781	19.8	7.2	-14.0	2.1	-23.4	10.0
19	242941	603252	15.7	6.3	-10.0	2.1	-15.1	9.8
504	254192	575265	-19.7	6.4	-5.0	2.1	-35.1	9.7
505	258044	579563	-7.3	7.3	-4.0	2.1	-19.6	10.1
507	246921	580984	-21.5	6.9	-5.0	2.1	-36.9	10.0
509	238841	586622	20.3	6.5	-8.0	2.1	-4.4	9.5
510	253583	589427	-29.0	6.8	-7.0	2.1	-50.6	9.7
511	245452	591161	5.5	7.3	-10.0	2.1	-25.4	10.0
512	260637	591947	19.5	6.9	-8.0	2.1	-5.2	9.9
513	242553	594974	4.9	6.1	-15.0	2.1	-41.4	9.2
514	231818	595421	-11.4	6.1	1.0	2.1	-8.3	9.2
516	250017	597182	12.4	7.9	-10.0	2.1	-18.5	10.7
518	254660	599568	11.6	7.2	-7.0	2.1	-10.0	10.7
520	227786	602778	7.3	7.2	-3.0	2.1	-1.9	10.2
521	237120	604985	23.6	6.3	-5.0	2.1	8.2	10.4
522	249275	607904	25.1	6.7	-9.0	2.1	-2.7	11.2

Table 3: Measured 1996-1978 time-lapse gravity changes and the corresponding error estimates. The numbers are rounded to the nearest decimal, Ref. [5].

Station	X (m)	Y (m)	Change in g (µGal)	Std. dev. g (µGal)	Change in z (cm)	Std. dev. z (cm)	Change in g, corrected (µGal)	Total error estimate for g corr., (µGal)
3	248512	567725	26.0	5.7	-8.0	1.7	1.3	11.3
8	234460	583093	27.4	4.1	-10.2	1.7	-4.1	9.4
15	238498	596425	26.0	5.9	-17.6	1.7	-28.3	10.2
17	243244	598781	40.1	6.0	-24.1	1.7	-34.3	10.3
19	242941	603252	36.2	5.2	-17.9	1.7	-19.1	10.2
504	254192	575265	-15.8	5.2	-12.7	1.7	-55.0	10.0
505	258044	579563	9.9	5.9	-10.8	1.7	-23.5	10.2
506	239019	578093	21.5	5.2	-8.1	1.7	-3.5	10.3
507	246921	580984	-12.4	4.8	-13.5	1.7	-54.0	9.9
509	238841	586622	61.3	4.8	-15.7	1.7	12.9	9.6
510	253583	589427	-15.0	5.3	-16.3	1.7	-65.3	9.8
511	245452	591161	8.0	6.1	-23.5	1.7	-64.5	10.2
512	260637	591947	18.7	5.6	-14.9	1.7	-27.3	10.2
513	242553	594974	38.9	5.3	-26.5	1.7	-42.9	9.8
514	231818	595421	12.2	5.3	-3.3	1.7	2.1	9.8
516	250017	597182	32.3	6.2	-21.7	1.7	-34.7	10.5
518	254660	599568	-31.9	6.0	-16.9	1.7	-84.0	10.9
520	227786	602778	13.1	5.9	-5.5	1.7	-3.9	10.4
522	249275	607904	12.5	5.5	-17.0	1.7	-40.0	11.4

Table 4: Measured 2015-1978 time-lapse gravity changes and the corresponding error estimates. The numbers are rounded to the nearest decimal.

3 Gravity data interpretation and scenario testing

To enhance understanding of what the data is telling, the measured time-lapse gravity changes were compared to synthetic gravity data which were generated using the dynamic reservoir simulation model.

3.1 Calculation methodology

Output from the V2.5 base case (2P) dynamic reservoir simulation model (BP2016 realization) was used to generate synthetic gravity data in Matlab. The static and dynamic reservoir data were provided on a 120 × 151 × 30 grid (NX × NY × NZ) and included:

- reservoir porosity,
- reservoir net-to-gross ratio,
- gas saturation,
- water saturation,
- gas density,
- water density,
- reservoir grid block volume,
- x, y, z-coordinates of the model grid centers.

The reservoir simulation data was extracted at several time intervals including those corresponding to analyzed gravity surveys, i.e., October 1978, February 1996, October 2015, and to optimize the planning of next gravity survey, also a few intervals running into the future, i.e., every two years from October 2019, October 2031. The reservoir data were subsequently exported as text files using the GSLIB file format and loaded into Matlab, where the gravity calculations were run using in-house developed codes. Details of the forward gravity modelling method are included in Appendix 1.

3.2 Modelled versus measured gravity changes

The total gravity change reflects net mass change i.e., a sum of (negative) mass change due to gas extraction and (positive) mass change due to water influx:

$$\Delta mass_{\,total} = \Delta mass_{\,gas} + \Delta mass_{\,water}$$

The gas production signal is generally dominating the total gravity change. To gain more insights into the individual contribution from these two components it is useful to analyze them separately.

From static and dynamic reservoir modeling, there is a fairly good handle on the initial gas column weight (product of reservoir thickness, net-to-gross, porosity, gas saturation, gas density), and on the depletion of the gas column in time (governed by reservoir pressure decline, which is constrained by over 1800 SPG measurements).

3.2.1 Model results

The modelled 1996-1978 gravity changes are shown in Figure 24 and Figure 25. The total gravity change ranges from approximately -31 to +1 μGal. By extracting the individual contributions from the water and the gas from the simulator, their respective contributions can be investigated. The maximum gravity change due to gas extraction is approximately -35 μGal (at station 516, Leermens). The maximum gravity change due to water influx is approximately +13 μGal at station 509 (Ten Boer). The (dedicated) water signal is spatially more heterogeneous than the gas signal and is visible mainly at the flanks of the field, where some aquifer support is expected.

Total gravity change

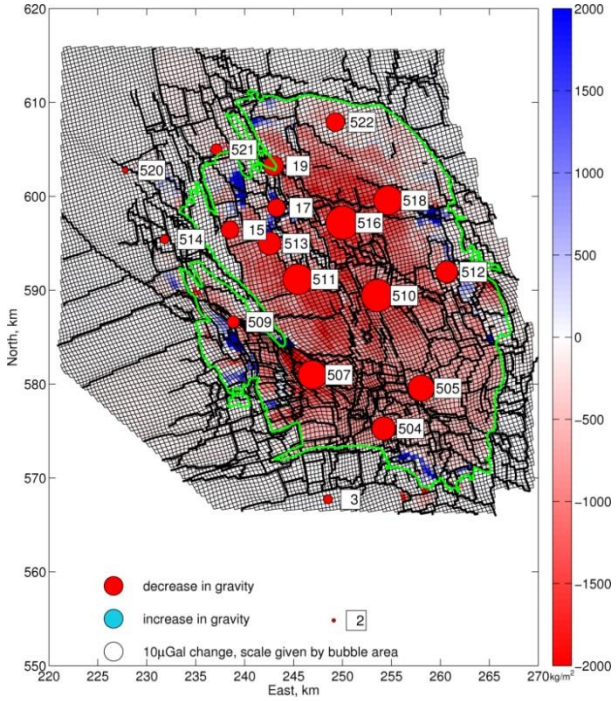

Gravity change due to gas extraction

Gravity change due to water influx

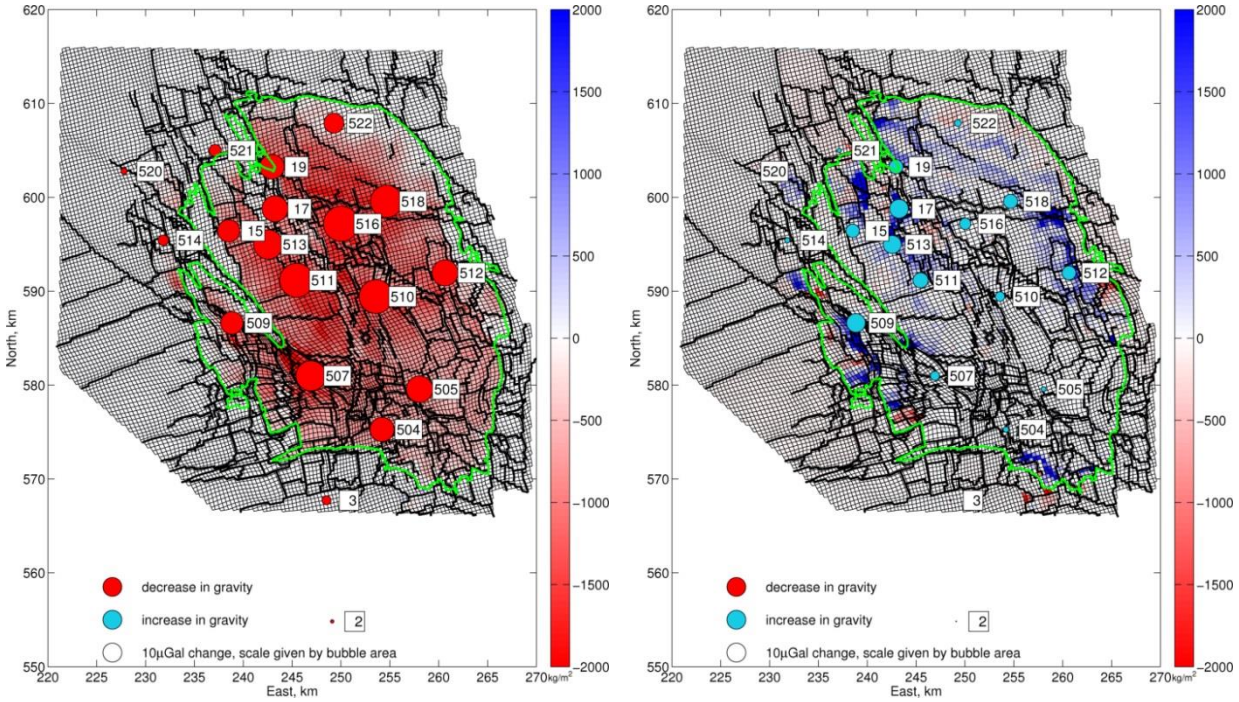

Figure 24: 1996-1978 reservoir mass changes (kg/ m2, sum over vertical column) and the corresponding modelled gravity changes (circles, where the circle size is proportional to the gravity signal magnitude). Top – total mass change; bottom left – mass change due to gas takeout; bottom right- mass change due to water influx.

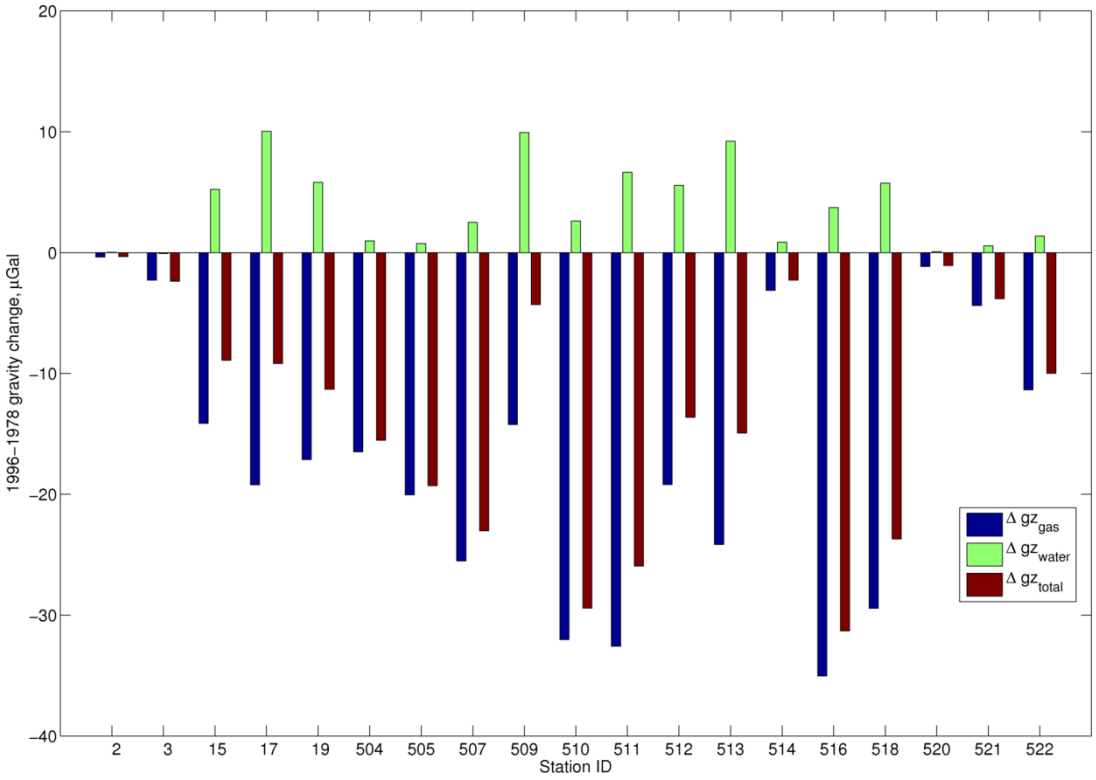

Figure 25: Modelled 1996-1978 time-lapse gravity changes. Gravity change due to water influx, due to gas takeout and the total signal, which is the sum of the two, are shown separately.

3.2.2 Comparing model results with measurements

A comparison of the modelled gravity changes to the actual measurements is shown in Figure 26 and Figure 27 for the 1996-1978 epoch. The mismatch varies from approximately -26 µGal to +14 µGal aligning into some patterns as can be seen from Figure 26.

At several stations the measured gravity reduction is larger than what is modelled (e.g., 15, 17, 513, 507, 510, 504). This could potentially be explained by:

- the reservoir model underestimating the mass of gas extraction from these areas,
- the reservoir model overestimating locally the amount of water influx,
- a combination of both.

Based on the geological knowledge and field measurements no significant water influx is expected (and modelled) in the vicinity of location Tussenklappen (stations 504, 507 and 510). Hence the first scenario of underestimating the gas takeout could be more applicable there. The second scenario might be more applicable in the vicinity of Stedum (stations 15, 17, 513) where some water influx is modeled.

In the North-East flank of the field the measured gravity reduction is smaller than what is modeled (e.g. nearby Bierum, stations 512, 516, 518, 522). This could be associated with more actual water influx than what is modeled.

The above scenarios will be tested in more detail in the following sections.

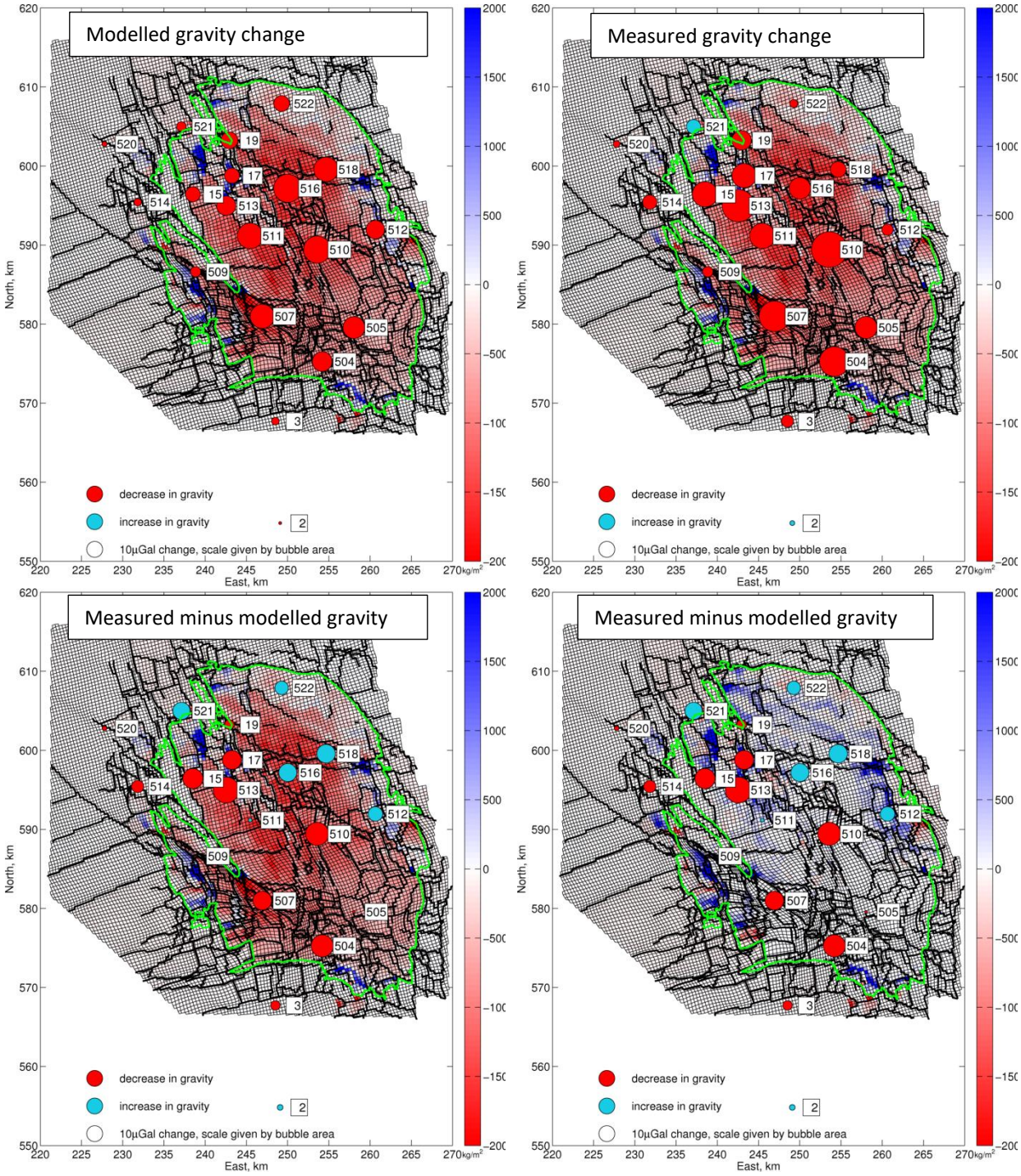

Figure 26: 1996-1978 reservoir mass changes (kg/m2, sum over vertical column) and the corresponding gravity changes shown with circles (top left-modelled; top right-measured; bottom -measured minus modeled). The circle size is proportional to the gravity signal magnitude. In the bottom right figure the reservoir mass changes due to water influx only are shown.

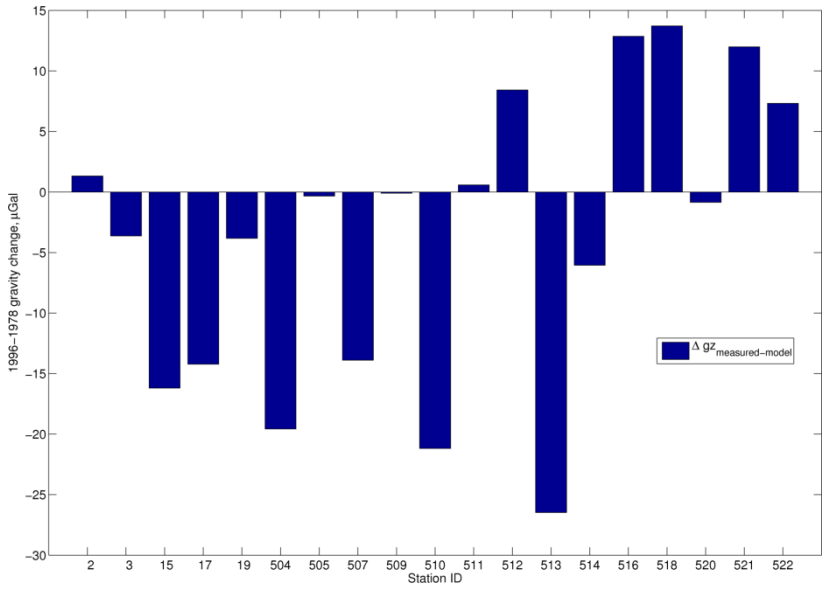

Figure 27: Measured minus modelled 1996-1978 gravity change.

3.3 Sensitivity analysis – Water influx in the North-East (1978-1996)

3.3.1 Overview of data and model result

An overview map with time-lapse measurements of the Gas-Water-Contact is shown in Figure 28. These measurements are based on interpretations of pulsed neutron density logging (PNL). A detailed overview of available PNL data can be found in Ref. [6].

A comparison of GWC rise from PNL measurements shows that the model under-predicts the measured GWC rise at the Bierum location. Figure 29 shows that between 1978-1996 there was approximately 12m of contact rise observed (Table 5), likely originating from the Rysum aquifer (Figure 1, see Ref. [6] for more information). The model on the other hand reflects no rise of the contact.

The difference between the measured and the observed gravity at station Bierum (518) is 14 µGal, suggesting that the model indeed needs more water influx in this area, which agrees well with the PNL data. The modelled gravity change due to gas take-off at Bierum, which is partly masking the water influx signal, is -29 µGal. Subtracting the modelled gravity change due to gas extraction (which is a smooth long wavelength signal constrained to production data using the reservoir model simulation) from the measured gravity change of -10 µGal yields an approximate water influx signal of +19µGal.

Due to uncertainties in aquifer connectivity, in the transmissibility of faults, and low confidence in some of the PNL measurements, the lateral extent of water influx around production location Bierum and the entire Eastern area of the field in general, remains uncertain (Figure 28). Gravity measurements sense the overall mass variations thus not only the changes taking place directly below the station but also in a certain station neighborhood. As a rule of thumb the signal decays with the distance squared between the observation point and the mass change source. Therefore, the measured gravity change provides some constraint on the lateral extent of water influx in the Bierum area.

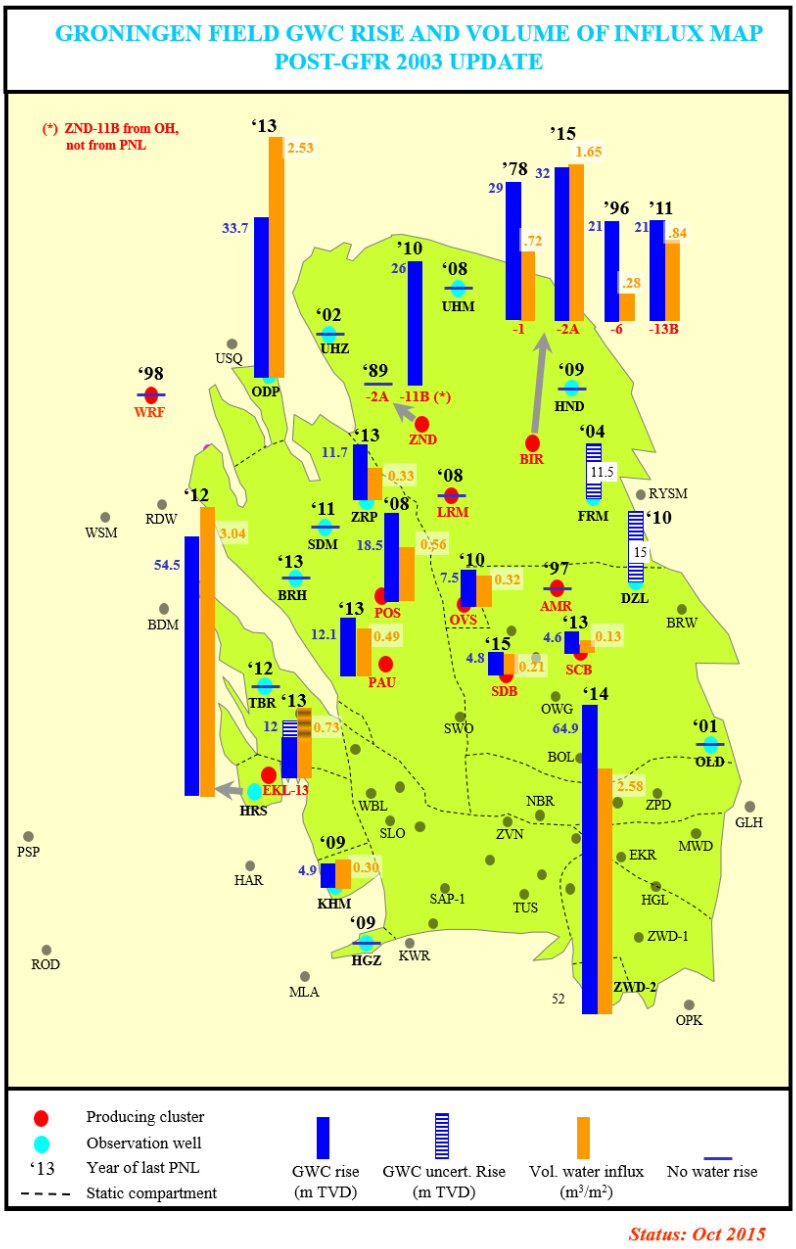

Figure 28: Groningen field GWC rise and volume of influx map. Status October 2015.

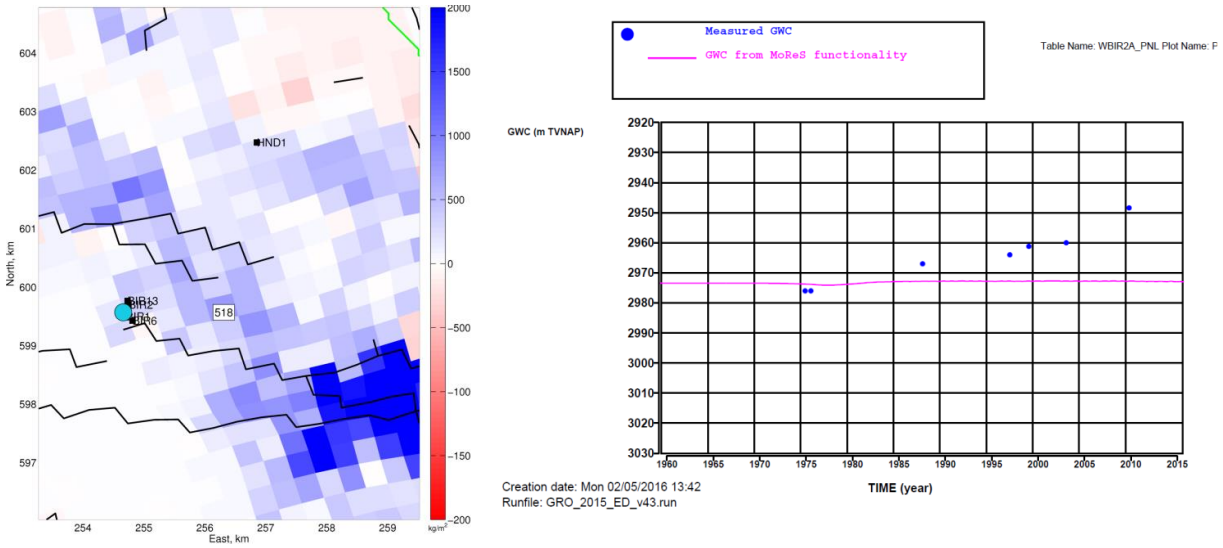

Figure 29: Zoom in at Bierum cluster area (left). Blue dot shows the location of gravity stations and black squares show the location of PNL wells. In the background 1996-1978 modeled mass change (kg/m2, sum over vertical) due to water influx is shown. The right plot shows a comparison of measured and modelled GWC rise at BIR-2A well.

Date	Tool	GWC		GWC Rise		Influx	
		(AH)	(TV)	(AH)	(TV)	(AH)	(TV)
28-Feb-75	OH	3061.7	2976.0	0.0	0.0	0.00	0.00
07-Oct-75	TDT/K	3061.7	2976.0	0.0	0.0	0.00	0.00
22-Jul-87	PDK	3052.3	2967.0	9.4	9.0	0.11	0.10
03-Oct-96	PDK	3049.5	2964.0	12.2	12.0	0.33	0.32
07-Oct-98	PDK	3046.3	2961.2	15.4	14.8	0.42	0.40
16-Sep-02	RST/A	3045.0	2960.0	16.7	16.0	0.29	0.28

Table 5: Measured GWC rise at Bierum (BIR-2A) location in 1975-2002 period. From Ref. [6].

3.3.2 Simple sensitivity analysis

A simple sensitivity test was run to understand how the time-lapse gravity measurements can constrain the spatial extent of water influx as seen at Bierum. For that purpose, a disk model was used to represent the water influx in this area. The disk thickness is equal to 12 m which is similar to the Bierum GWC rise measured over the 1978-1996 period. A density contrast of 80 kg/m^3 is assigned to this disk, based on the average density change for water replacing gas in the 1978-1996 period, as determined from the dynamic reservoir model simulation. The disk radius is varied and the synthetic gravity response at Bierum station is calculated (Figure 30).

The results show that time-lapse gravity can provide information on the spatial extent of water influx around Bierum. The base case fit of the disk size representing the flooded area is 5km and taking into account the average data uncertainty of 10μGal, the disk radius could range from 2.5 to 10 km. Increasing the disk radius further, say above 15 km, leads to a very limited increase in the modelled gravity response, as it approaches then the gravitational effect of Bouguer plate. In other words, 15km can be seen practically as a "saturation" or maximum radius beyond which the gravity measurement at Bierum has very limited power to further differentiate the extent of the water influx area.

When evaluating the sensitivity results of the disk model with respect to the spatial extent of the field, to the size of fault compartments which could potentially constrain the aquifer ingress, and to the distances between the gravity stations, it appears that the water influx as observed at the Bierum station shall also be detected by adjacent gravity stations e.g., Leermens (516). This means that the gravity results must be mutually consistent

which gives more robust QC options helping to build confidence of interpretation and scenario testing to follow (Figure 31).

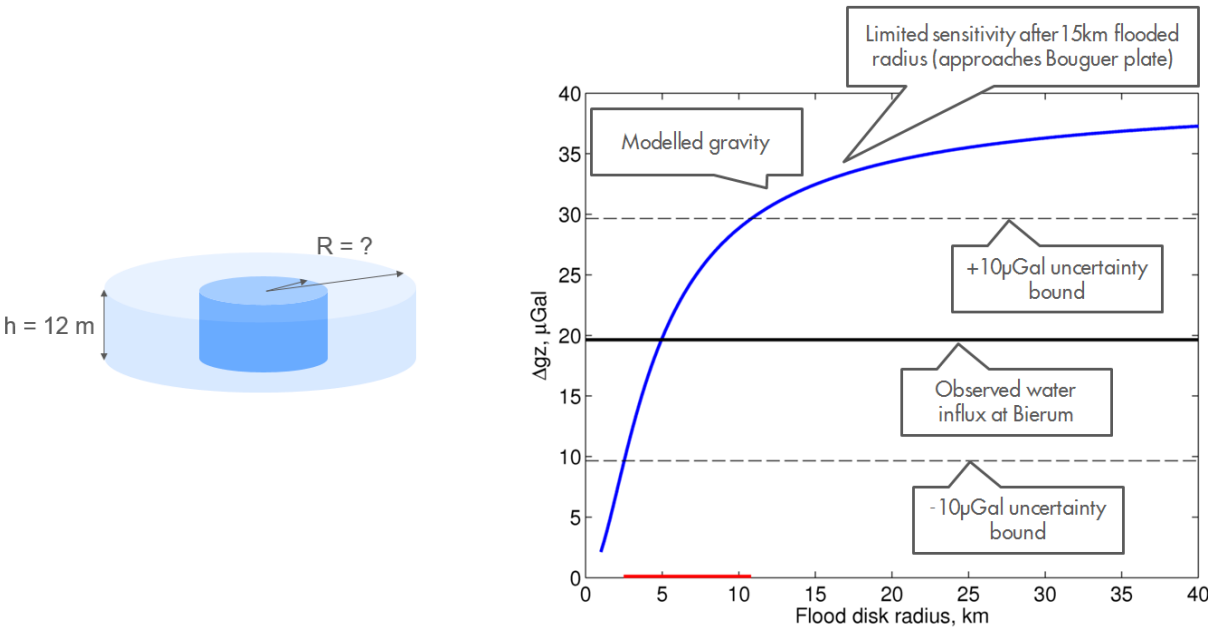

Figure 30: Sensitivity testing for 1996-1978 water influx at Bierum with water flood disk model.

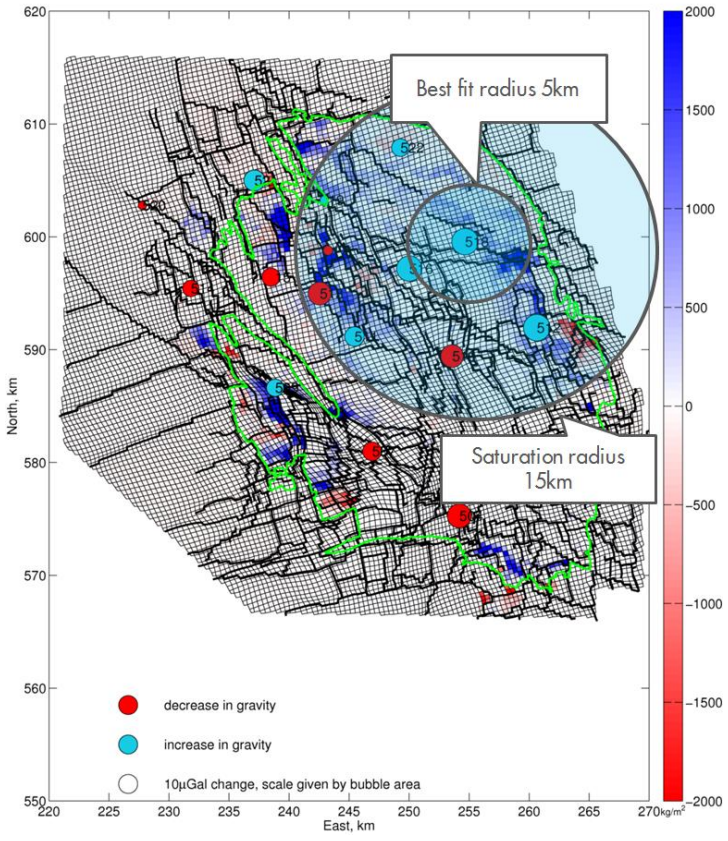

Figure 31: Bierum 1996-1978 water influx sensitivity testing results. In the background modeled mass change due to water influx for 1978-1996 period are shown. Circles show 1996-1978 measured gravity change corrected for the modelled gravity attraction due to gas takeout.

3.3.3 Regional sensitivity analysis

More detailed sensitivity tests for water influx scenarios were done using additional gravity stations within the area while honoring PNL measurements in nearby wells as further constraints (Figure 32).

The modeling is testing various lateral extents of the observed 12 m GWC rise at Bierum with an associated 80kg/m³ density change due to water replacing gas. The areal extend of the water influx is however constrained by the geometry of fault blocks, and does honor the PNL data from the adjacent wells. The tested geometries are converted into mass change, and inserted into the modelled mass change grid.

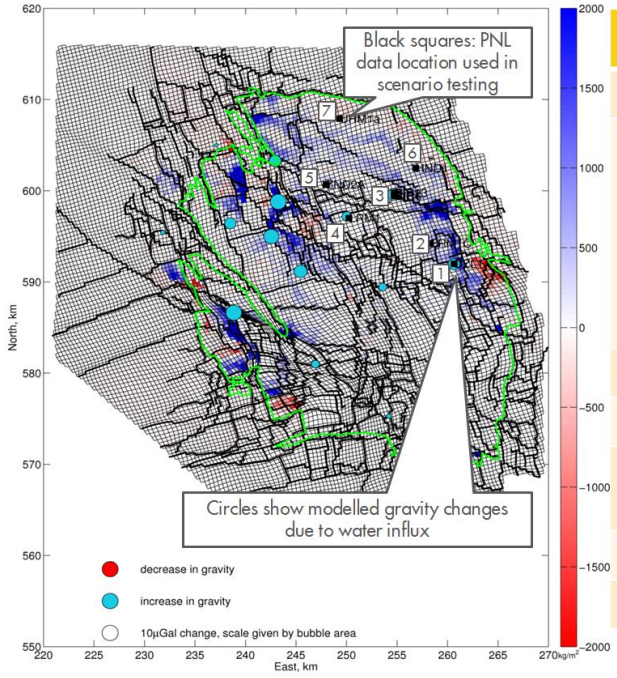

	Well	1978-1996 GWC rise	Confidence	GWC rise after 1996?
1	DLZ-1	~5m	Poor	Yes
2	FRM-1C	-	No measurement in 1978 (first reading in 1990). Since then GWC rise seen but uncertain.	Yes
3	BIR-2A	12m	Good	Yes steady
4	LRM-7	0m	Moderate	No
5	ZND-2	0m + ?	Good, no measurement around 1996	Yes
6	HND-1	0m	Good	No
7	UHM-1a	0m	Moderate	No

Figure 32: An overview of PNL data used to constrain the 1996-1978 water influx scenario testing in the North-East of the field.

Reference case

Figure 33 shows the reference case in the scenario testing, i.e., the modelled mass change due to water influx based on the reservoir model simulation for the 1978-1996 period with the corresponding modeled gravity changes and observed gravity changes corrected for modelled gas takeout effect. The ±10 μGal average uncertainty bounds are added to the plots. Four gravity stations are highlighted where the observed gravity consistently suggests more water influx compared to the model.

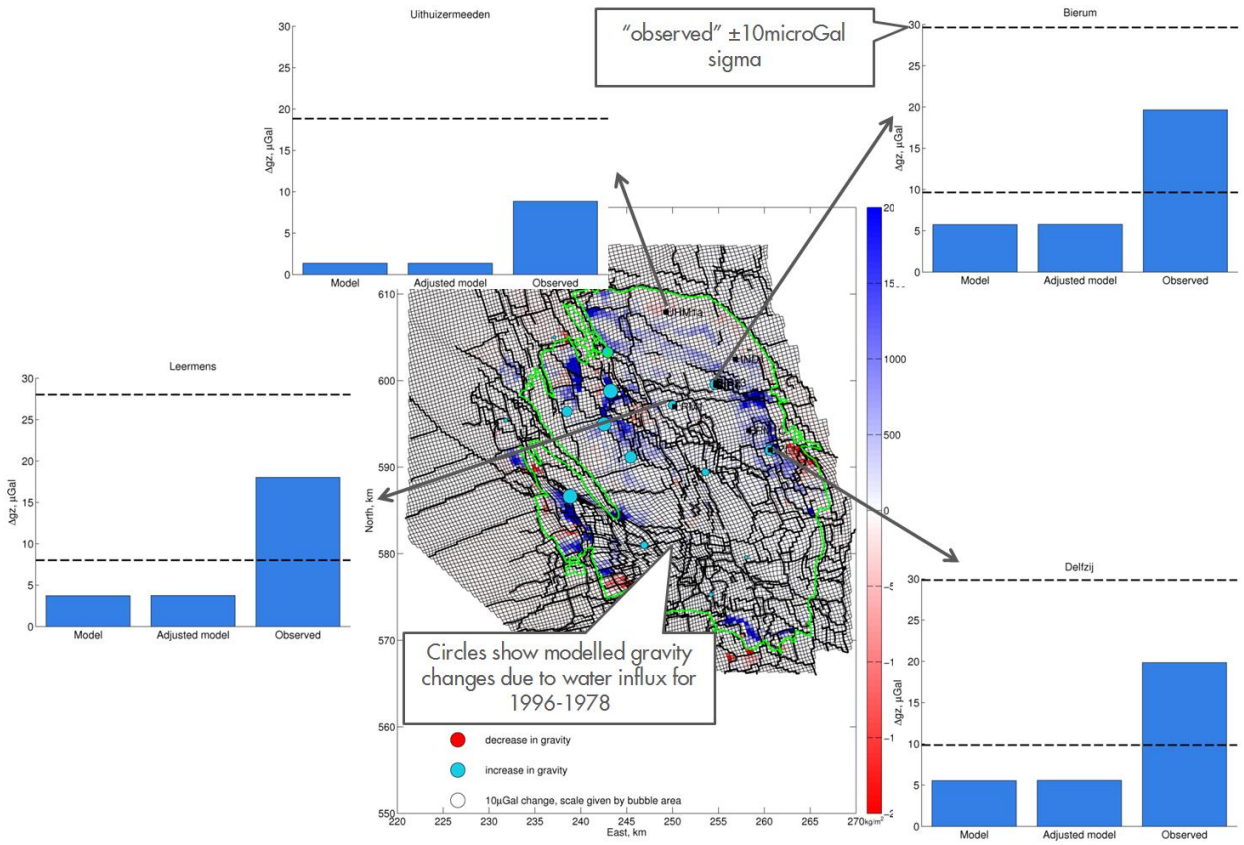

Figure 33: Starting point for the 1996-1978 water influx scenario testing in the North-East of the field showing the modelled and the measured gravity effect due to water influx. In the background modelled mass change due to water influx is shown (kg/m2, sum over vertical column) with the corresponding modelled gravity change (circles).

Scenario #1

Scenario #1 examines the impact of a synthetic 12m water influx across the entire fault block encompassing the Bierum production cluster (Figure 34). In this case gravity change from the adjusted model gets clearly closer to the measured gravity change but still seem to be too low. Figure 35 shows the size of flooded compartment in relation to the sensitivity testing results.

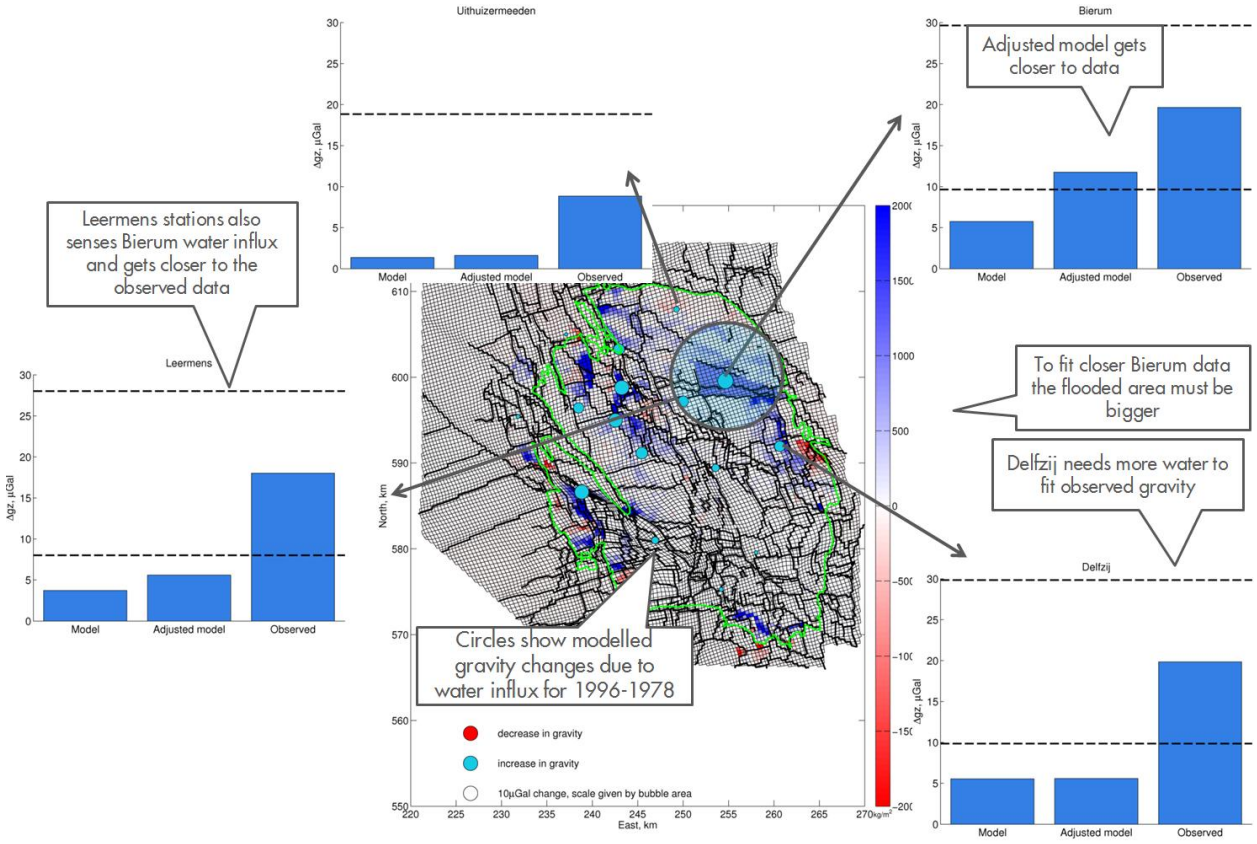

Figure 34: 1996-1978 water influx scenario #1 in the North-East of the field. The modelled and the measured gravity effect due to water influx is shown. In the background the modelled mass change due to water influx in the adjusted model is shown (kg/m2, sum over vertical column) with the corresponding modelled gravity change (circles).

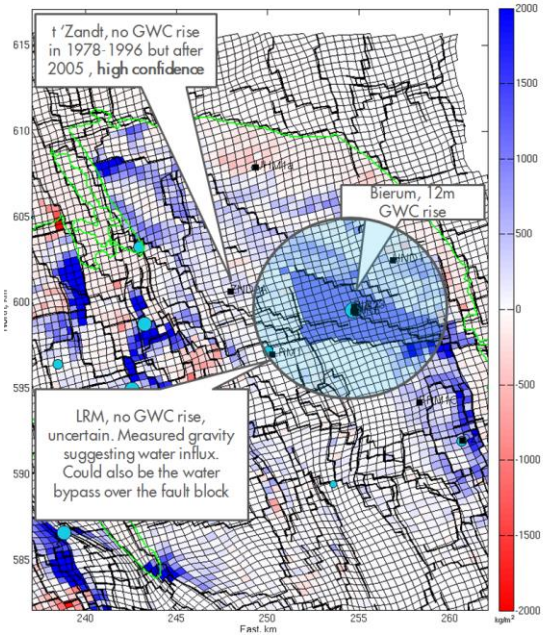

Figure 35: Zoom in in the 1996-1978 water influx scenario #1 around Bierum area. The circle shows best fit 5km radius of flooded area explaining Bierum gravity data.

Scenario #2

Scenario #1 shows that there is still insufficient water influx to match the observed gravity change at all the stations. The associated change in the gravity signal resulting from Scenario #1 extended to station Leermens, which is a few kilometers away. The best fit from the simple disk model sensitivity was at a 5km radius, suggesting a larger areal extend than the flooded block in Scenario #1.

A further sensitivity (Scenario #2) was defined to test a much larger extent of the water influx, covering most of the North-Eastern area (Figure 36). The areal extent was chosen such as to be consistent with the measured GWC rise observed from PNL logging of the wells in the area (Figure 37). In this case the match to the observed gravity change is much better with adjusted model gravity getting close the observed gravity change.

Due to data availability, the scenario testing was only performed for 1978-1996 period, for simplicity the same 12 m GWC rise was assumed within the tested area. How the water influx could evolve after 1996 remains to be tested with reservoir model simulations. The scenarios considered are non-unique due to the limited spatial resolution of gravity data. This means that there might be more scenarios with slightly different shape of water influx still honoring gravity data. Tested scenarios however, provide useful insights on what is needed to explain gravity data. The learnings from here can then be taken to the next phase based on assisted-history matching combining gravity with other surveillance data.

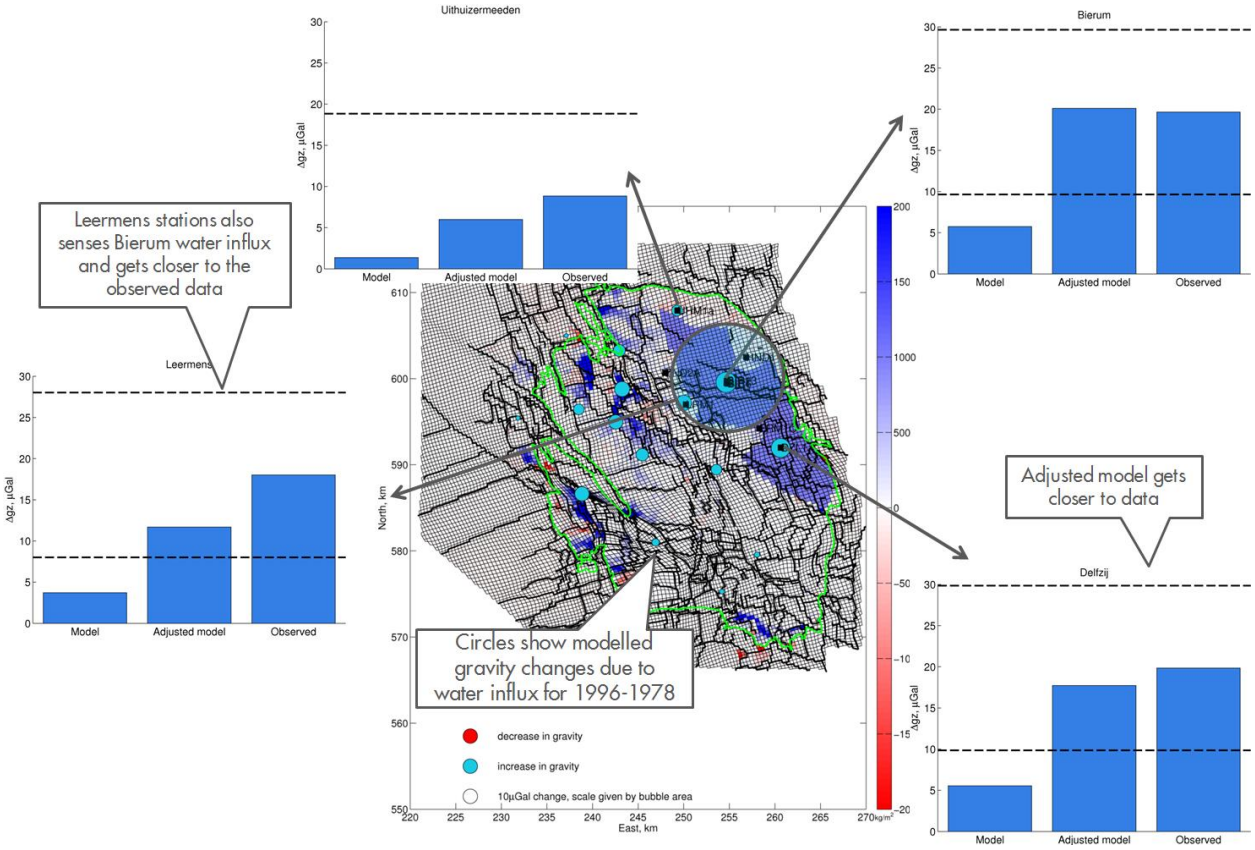

Figure 36: Water influx scenario #2 fitting the observed 1996-1978 gravity data and consistent with measured GWC rise at PNL wells. The modelled and the measured gravity effect due to water influx is shown. In the background the modelled mass change due to water influx in the adjusted model is shown (kg/ m2, sum over vertical column) with the corresponding modelled gravity change (circles).

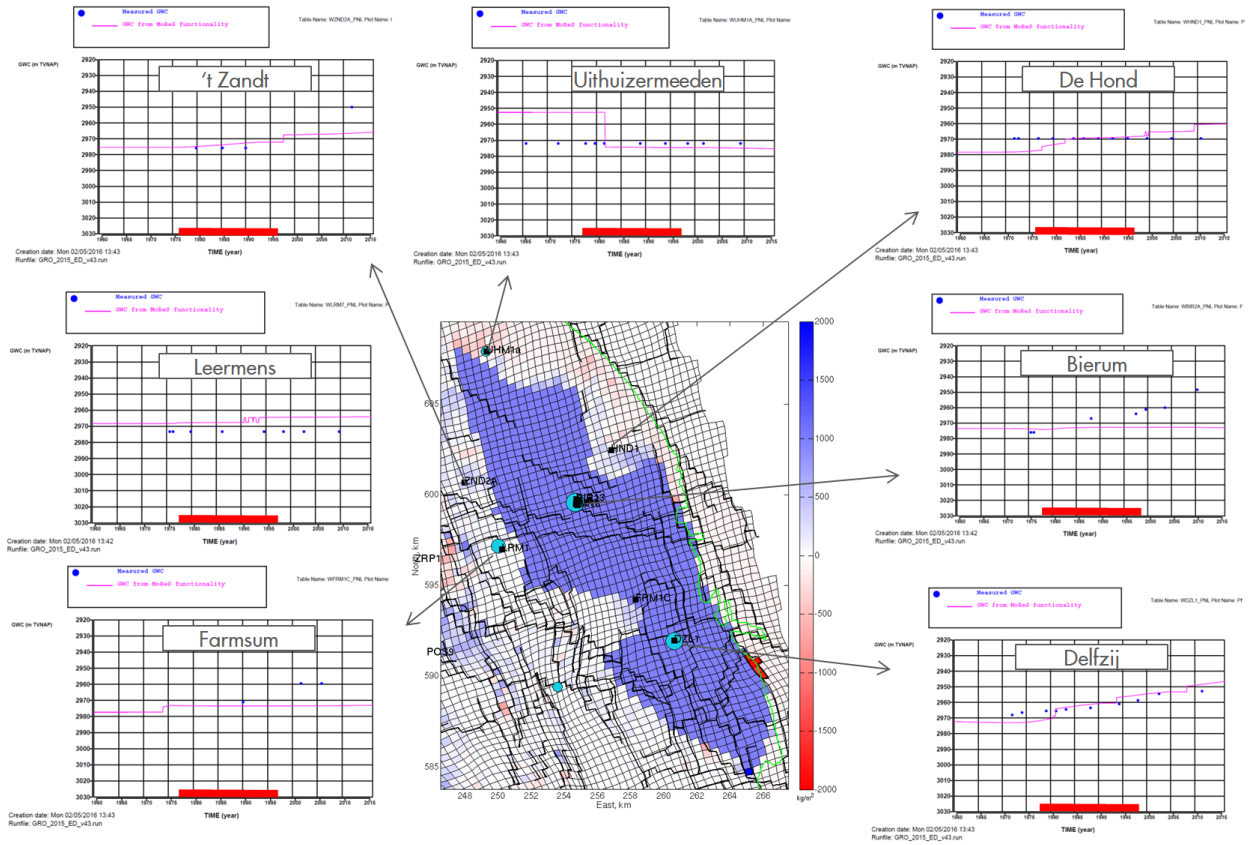

Figure 37: Water influx scenario #2 compared to PNL measurements. Red bar highlights the analyzed period 1978-1996.

3.4 Sensitivity analysis – Water influx in the South-West

Another area where comparison of modelled vs observed gravity shows a consistent mismatch at a few stations is nearby Stedum (e.g. stations #15, #15, #513), see Figure 26. In this case the mismatch is of opposite sign as compared to Bierum area, with observed gravity suggesting more mass reduction/less water influx than currently modelled. This is consistent with PNL measurements, which show that the reservoir model overpredicts the measured GWC rise nearby Stedum (Figure 38). The opposite can be seen nearby Usquert at station #521 where gravity suggests more water than currently modelled. This seems to be in-line with the PNL measurements. At location Oldorp (ODP1) the model clearly underestimates the measured GWC rise. Overall the water influx scenarios around Stedum could be complex due to uncertainty in the transmissibility of faults in this area. In this section, we will consider simplified cases indicating only which case could explain better the measured gravity change. The approach will be similar to the one applied for testing water influx scenarios nearby Bierum. Here however, we will reduce the modelled water influx rather than increase it. This will be done by "muting" the mass changes related to the water replacing gas. There are three stable gravity stations which did not need to be transferred in 2015: Middelstum church (#15), Garsthuizen (#17) and Uithuizermeeden church (#19). Thus 2015-1978 gravity change from these stations is not affected by additional uncertainties due to the transfer and will be used in the analysis. Station Stedum (#513) had to be re-established in 2015 as the observation hut in which the gravity point was located was

removed early 2000. No uncertainty exists regarding the measurement location as the outline of the observation hut is still visible on the asphalt surface (Figure 39). The new 2015 measurement point was established at 1-2 m distance from the original location thus there are no uncertainties related to the gravity gradient measurements. The main source of the uncertainty is a possible change in height, as the previous point was on a hut floor, of which the exact height above the surface remains uncertain. We will still plot Stedum 2015 gravity data, keeping in mind the above.

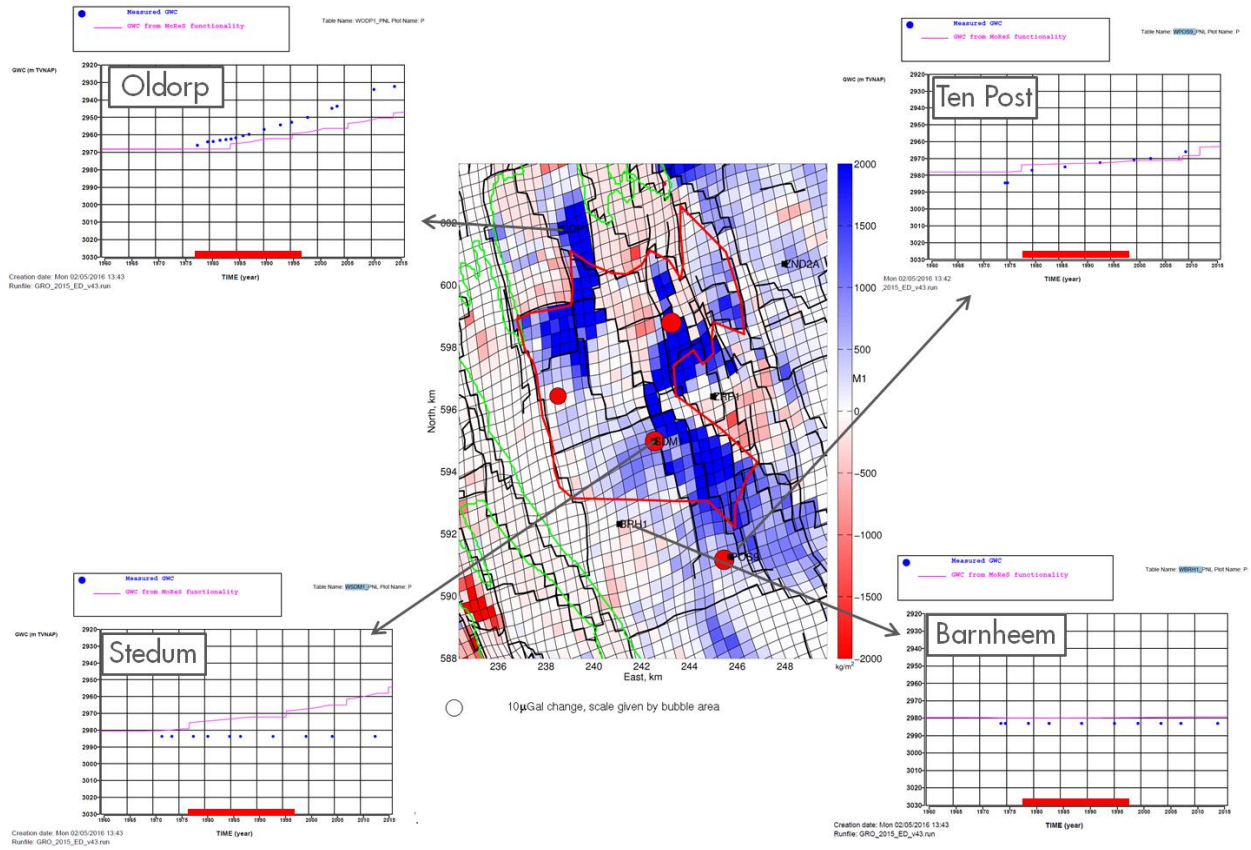

Figure 38: GWC rise from PNL wells compared to reservoir model predictions. The middle plot shows the 1996-1978 mass change (kg/m2, sum over vertical column) in the water phase. Circles show the difference between 1996-1978 observed and the modelled gravity change (red-negative, blue positive).

Figure 39: Station Stedum (513). An outline of observation hut where gravity was measured in the past is still visible in the surface. The 2015 gravity measurement was taken in close vicinity of original location. Photo Ref. [5].

The modelled scenario with water influx removed is shown in Figure 40. A much improved fit to the measured gravity changes is obtained, especially at station Garsthuizen where the model follows the data very closely after the adjustment. Uithuizermeeden church station shows minor changes indicating that the model is already in a good agreement with the measurements there. Station Middelstum church and Stedum show improvement as well but have approximately 10 μGal residual mismatch remaining in 1996. This could be attributed to insufficient detail in modelling applied here, data uncertainty or other factors, such as more mass reduction due to gas takeout in this area in 1978-1996 period than currently modeled.

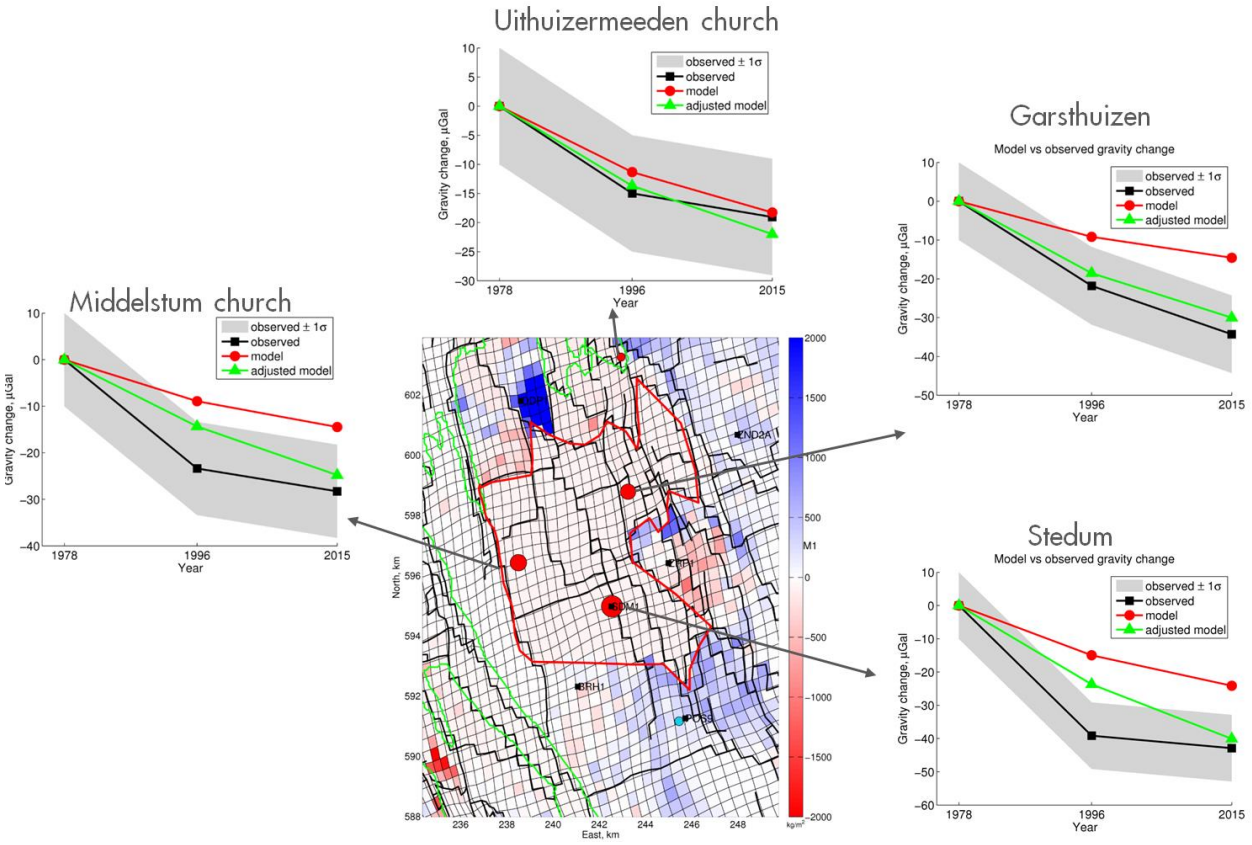

Figure 40: Testing water influx scenario near Stedum. The middle plot shows 1996-1978 mass change due to water influx as predicted by reservoir the model and modified within red polygon where the water influx is removed. The same was applied to 2015-1978 mass change (not shown here). The corresponding gravity changes, before and after the model modification, are shown with time series plots and are compared to the observed gravity change. The grey band shows the observed gravity ±10μGal average uncertainty range.

3.5 Sensitivity analysis – Carboniferous depletion

3.5.1 Geological setting

The Slochteren Sandstone reservoir is overlying rocks of Carboniferous age, with the interface formed by an angular unconformity (Figure 41). A limited number of (extended) wells have been drilled into the Carboniferous. These have indicated a lithology dominated by shales, with variable amounts of interbedded sandstone and coal beds. In combination with the varying structural dips, there is a high uncertainty in the 3D distribution of rock types in the Carboniferous.

In the south of the Groningen field, the upper part of the Carboniferous sequence extends above the Groningen gas-water-contact, and hence is gas-bearing. Its reservoir properties have been investigated in a petrophysical study, Ref.[9]. An overview of the main results is given in Figure 42. Sandstone layers were observed up to 40m in thickness with porosities up to 13% and hydrocarbon saturations up to 70%, (wells ZVN-2, KPD-1 and EKR-9). Detailed mapping of intra-Carboniferous reflectors is prohibited by the limited quality of the seismic imaging.

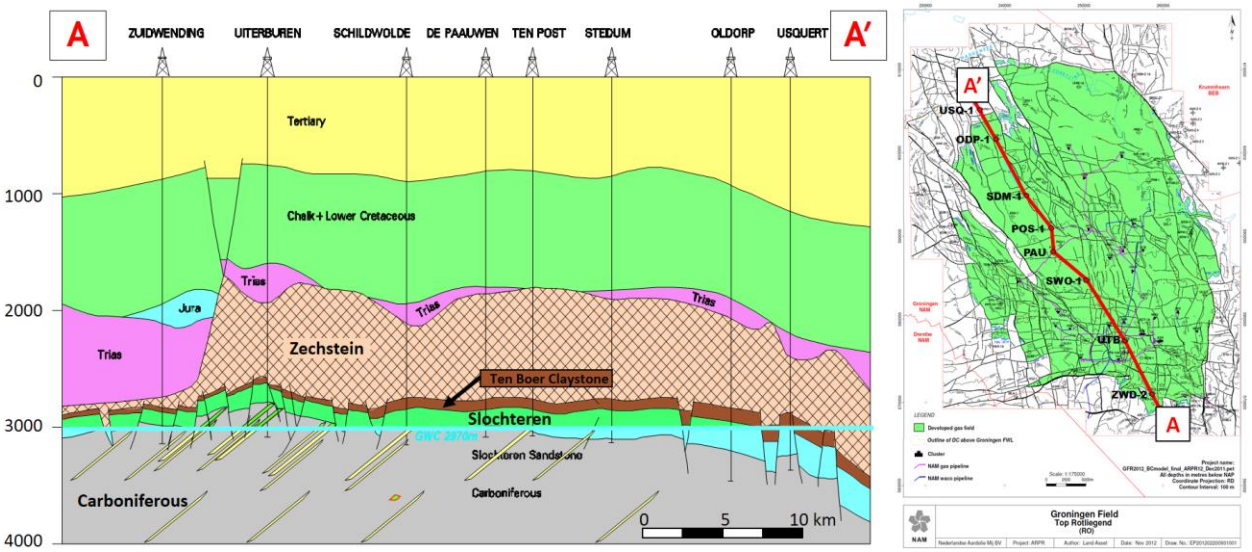

Figure 41: Geologic cross section through the Groningen field.

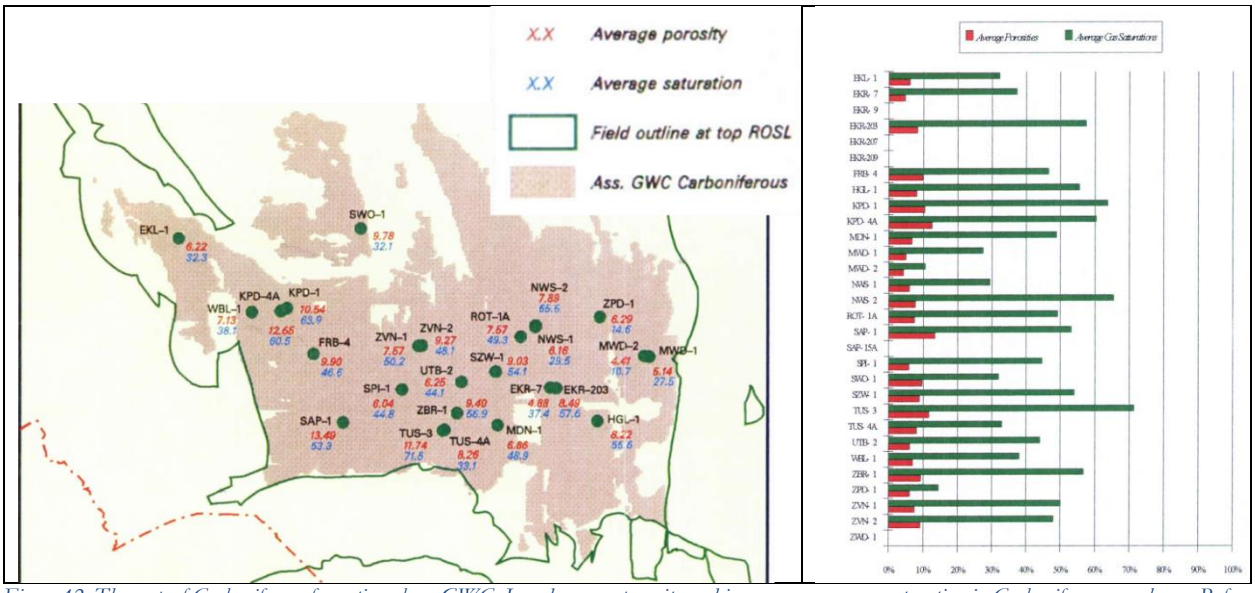

Figure 42: The map of Carboniferous formation above GWC. In red average porosity and in green average gas saturation in Carboniferous are shown. Ref. [9].

3.5.2 Depletion

Figure 43 gives an overview of all pressure measurements within the part of the Groningen field where the Carboniferous is gas-bearing. The dataset is dominated by Slochteren pressures, which show a fairly uniform depletion throughout the area. Over the period 1978-1996, Slochteren pressure declined from 240 to about 155 bar, yielding a depletion of roughly 90 bar. The period from 1996 showed an additional 80 bar depletion, to a reservoir pressure of some 75 bar.

There is limited pressure data available from the Carboniferous, and the lateral extent of any measured depletion is unclear. Depletion of the Carboniferous sands has been demonstrated in some wells. There is no dedicated production from the Carboniferous, which indicates pressure communication with the main Slochteren Sandstone reservoir. Observation well Heiligerlee-1 has only been perforated in the Carboniferous (up to 2012). It can be seen from Figure 43 that it consistently lags some 20 bars in pressure with respect to the overlying Slochteren pressure. However, due to the poor reservoir quality (low permeability) and consequently slow build-up of reservoir pressure, there is some ambiguity in the pressure lag. Ref. [12] describes a pressure measurement in Feb 2007. The highest measured pressure was 139 bar (at datum, 2875mTVDSS). However, given that the pressure was still building up after a month, the extrapolated reservoir pressure was estimated to be 190 bar. The estimates for the pressure lag in this particular perforated sand body therefore vary between 20 and 70 bar. It is likely that the Carboniferous pressure field is highly variable, showing more depleted and less depleted intervals, which cannot be resolved from the available data.

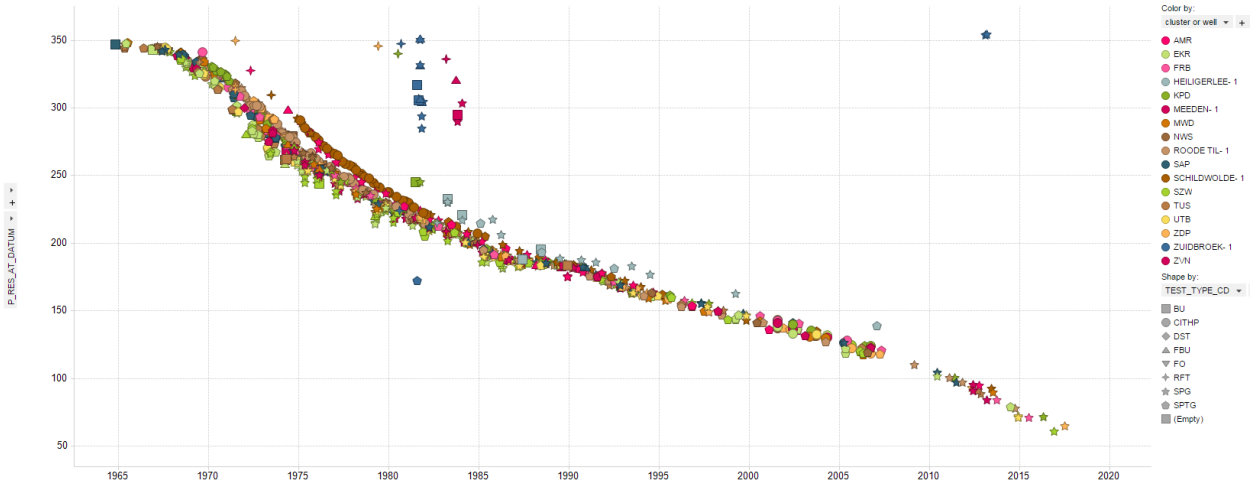

Figure 43: Overview of reservoir pressure measurements from all wells within the Carboniferous closure as indicated in Figure 42.

3.5.3 Gravity data

Figure 44 shows that the model under-represents the observed gravity change in the South of the field. There are three gravity stations within the area with stable time-lapse data, which consistently show that more mass should be extracted from the model.

The Carboniferous is not included in the (V2.5) dynamic reservoir model. The extent of the gas-bearing Carboniferous is indicted by the red polygon in Figure 44. The pressures in the Slochteren overlying the Carboniferous are matched within 2 bar, which means the density, and with that the mass, within the Slochteren reservoir is well constrained. Because the Slochteren formation is well above the contact, and no water influx is expected from the Carboniferous due to its very low permeability, there is no water influx modeled. Hence, only additional pressure depletion, could explain the difference. Pressure depletion is linked to gravity changes via induced mass reduction, i.e. reduced pressure will lead to a decrease in gas density due to expansion and eventually to mass decrease. It is assumed that the pressure depletion in the Carboniferous, which is not included in the dynamic models, is the cause of this difference.

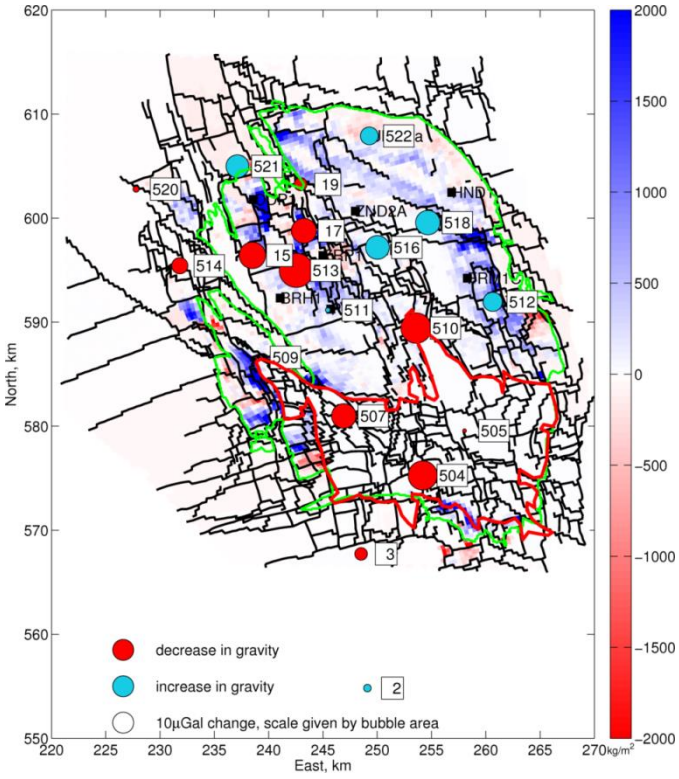

Figure 44: 1996-1978 observed minus modeled gravity difference. In the background modelled mass change due to water influx is shown (kg/m2, sum over vertical). Red polygon shows the Carboniferous outline where gas could be depleting.

3.5.4 Sensitivity analysis

The potential depletion of the Carboniferous was tested with synthetic scenarios. A 3D model was built to investigate the impact of a potential mass reduction in the Carboniferous. The Matlab grid which is used to evaluate the mass changes as obtained from the dynamic reservoir simulation model was locally expanded in the South to include the depleting Carboniferous formation (Figure 45).

In light of the combined uncertainty in net sand and depletion, it was assumed that the entire Carboniferous closure can be represented as a homogeneous tank, e.g. using single parameters to reflect average static and dynamic properties.

Two sensitivities were tested, varying both the static properties and the pressure depletion estimate (Figure 46, Tables 6 and 7). The change in gas density as a function of pressure depletion is given in Figure 47. In order to bridge the mismatch in the gravity change, fairly extreme reservoir properties were assumed with respect to the (limited) dataset as described in section 3.5.1.

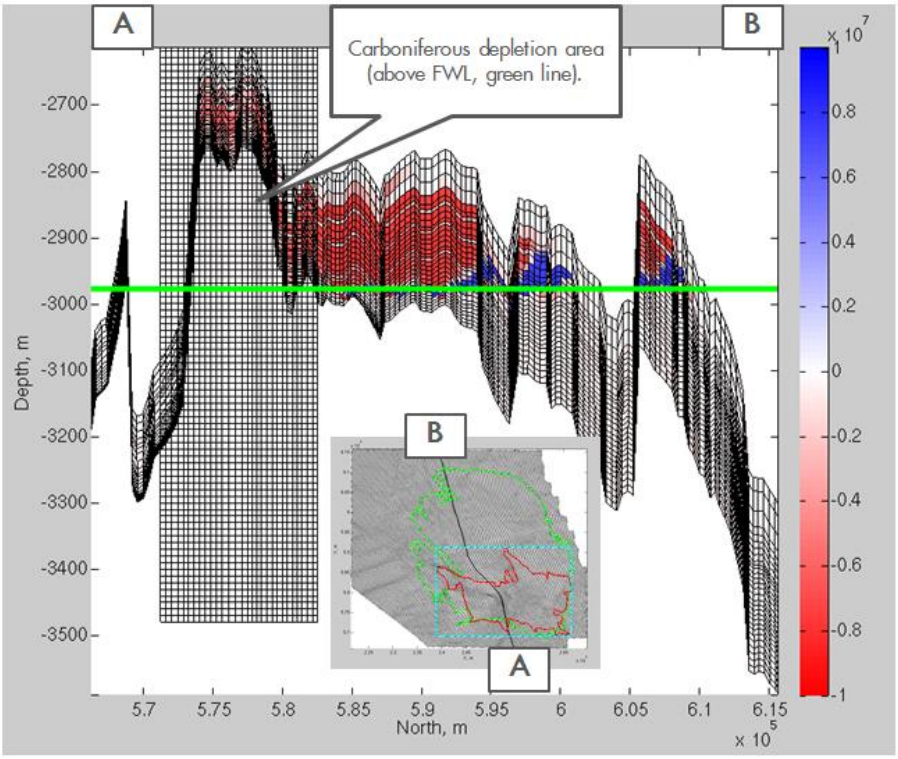

Figure 45 :Model setup for testing Carboniferous depletion scenarios with gravity. 1996-1978 reservoir model mass change (kg) is shown. Additional grid is inserted to model depletion within Carboniferous (above FWL, green line).

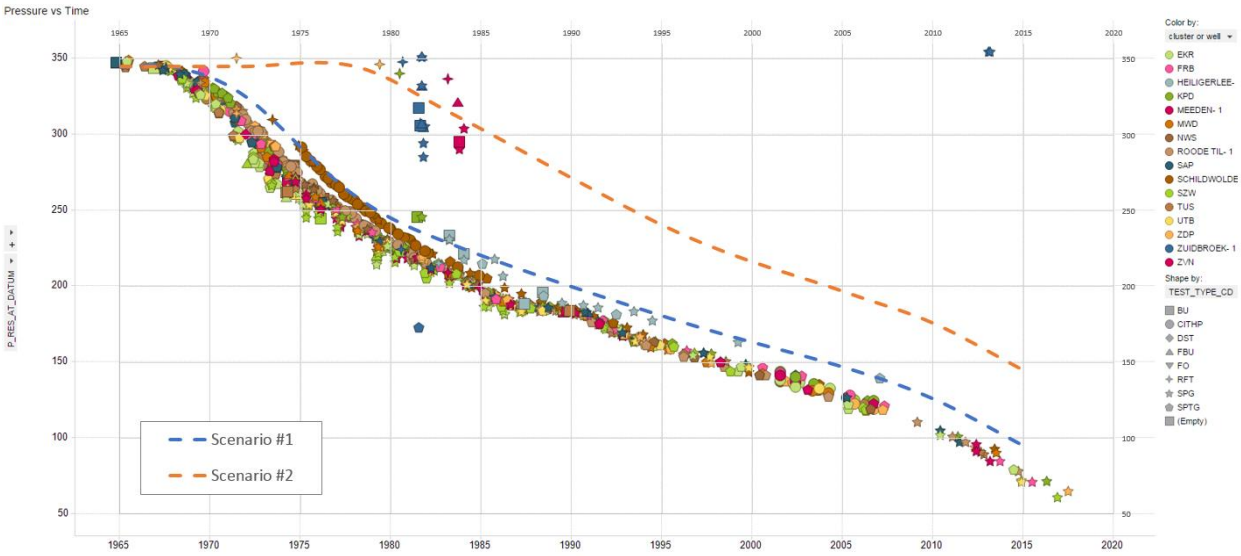

Figure 46: Pressure lag scenarios

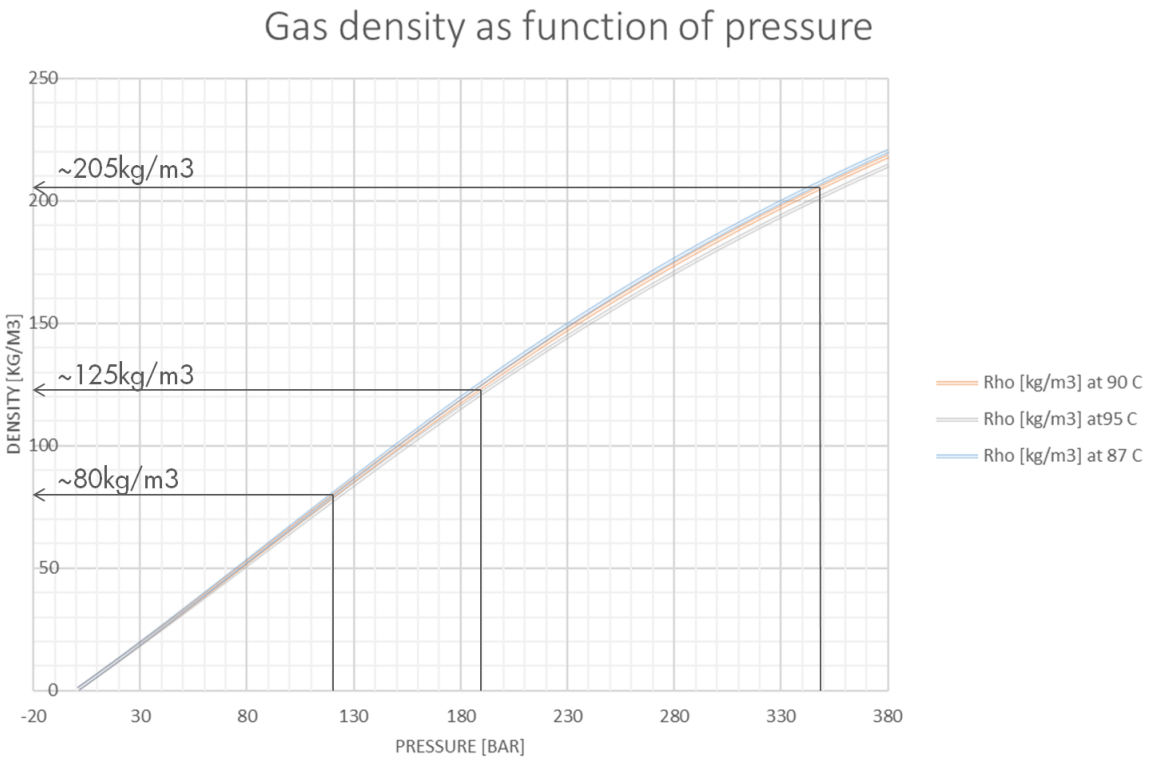

Figure 47: Gas density vs reservoir pressure for Groningen field.

Scenario #1

Table 6 gives the assumed static and dynamic parameters as used in Scenario #1. The associated bulk density change in the Carboniferous is approximately -1.2 kg/m³ for both epochs.

year	ϕ	Sg	N/G	pressure Slochteren (bar)	pressure Carboniferous (bar)	gas density Carboniferous (kg/m³)	bulk density gas (kg/m³)	
1978	9%	50%	50%	240	240	153	3.4	
1996	9%	50%	50%	157	157	103	2.3	
						bulk density change:	**-1.1**	**kg/m³**
1996	9%	50%	50%	157	157	103	2.3	
2015	9%	50%	50%	75	75	46	1.0	
						bulk density change:	**-1.3**	**kg/m³**

Table 6: Assumed Carboniferous static and dynamic parameters and associated bulk density change for Scenario #1, over the period 1978-1996 and 1996-2015

Scenario #2

Table 7 gives the assumed static and dynamic parameters as used in Scenario #2. The associated bulk density change in the Carboniferous is approximately -1.7 kg/m³ for both epochs.

year	ϕ	Sg	N/G	pressure Slochteren (bar)	pressure Carboniferous (bar)	gas density Carboniferous (kg/m³)	bulk density gas (kg/m³)	
1978	13%	50%	50%	240	345	203	6.6	
1996	13%	50%	50%	157	235	150	4.9	
						bulk density change:	**-1.7**	**kg/m³**
1996	13%	50%	50%	157	235	150	4.9	
2015	13%	50%	50%	75	145	96	3.1	
						bulk density change:	**-1.8**	**kg/m³**

Table 7: Assumed Carboniferous static and dynamic parameters and associated bulk density change for Scenario #2, over the period 1978-1996 and 1996-2015

Discussion of results

Due to the relatively low porosity and net-to-gross in the Carboniferous, the overall bulk density changes are low compared to the Slochteren reservoir, which has bulk density changes in the gas bearing column in the order of -8kg/m^3 over the 1978-1996 period.

The modelled gravity changes between 1978-1996 caused by depletion of the Carboniferous are given in Table 8.

Gravity station	Scenario #1	Scenario #2
504	-6.3	-8.4
507	-4.4	-5.5
510	-2.5	-2.9

Table 8: Modelled gravity change (μGal) between 1978-1996 resulting from depletion of the Carboniferous

The model response for Scenario #1 and Scenario #2 as compared to the observed gravity change for stations 504, 507 and 510 is shown in Figure 48 and Figure 49. The results show that depletion in the Carboniferous reduces the mismatch between modelled and observed gravity change, with Scenario #2 fitting the data slightly better. Station Schildmeer (510) is located at the far edge of the Carboniferous closure, and is thus only impacted to a limited degree by depletion of the Carboniferous. The biggest improvement can be seen at station Tussenklappen (504).

The mismatch was not fully resolved, which could be a reflection of the simplified modelling approach and the data uncertainty. Because all three stations were transferred in 2015, there is additional uncertainty in the measured 1978-2015 gravity change, which is not fully reflected by the displayed error band.

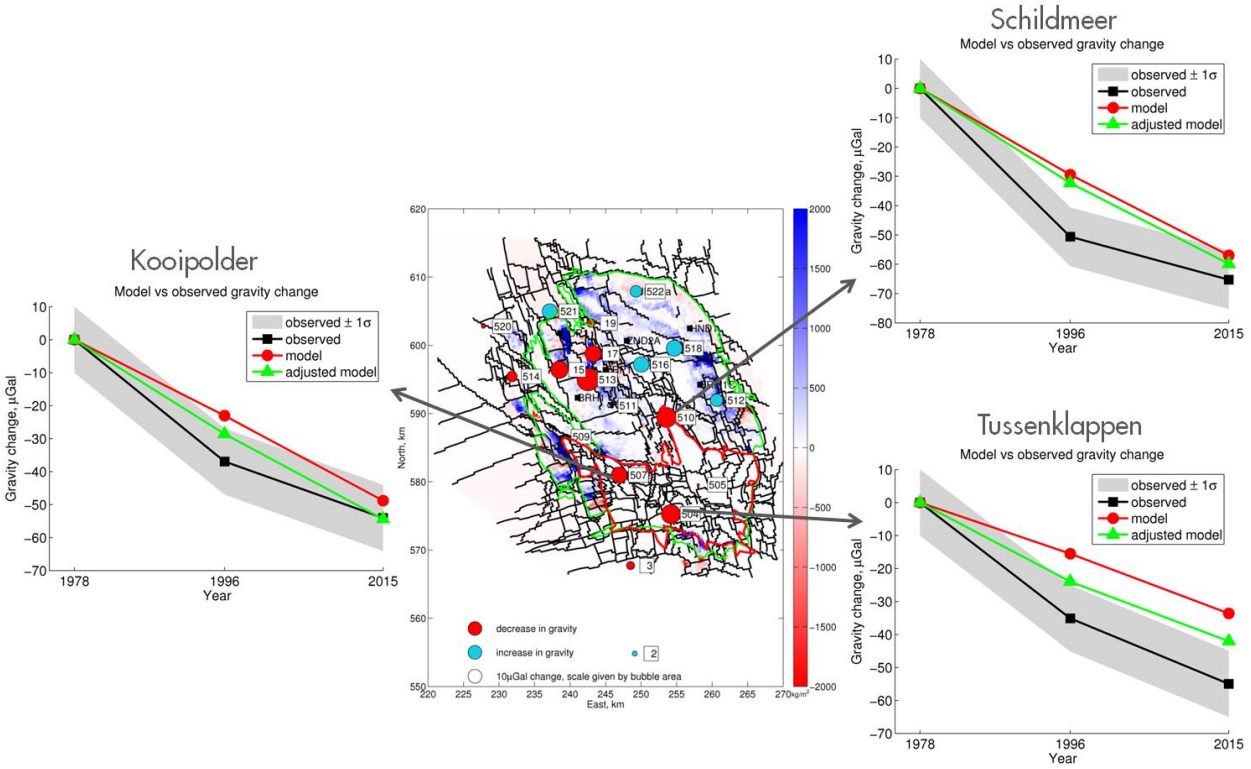

Figure 48: Scenario #1 – Modelled vs observed gravity change (time-series plots, the total signal is shown) for Carboniferous depletion. The middle plot shows 1996-1978 modelled mass change for water (kg/ m², sum over vertical column) with the observed minus modelled gravity difference for the same period.

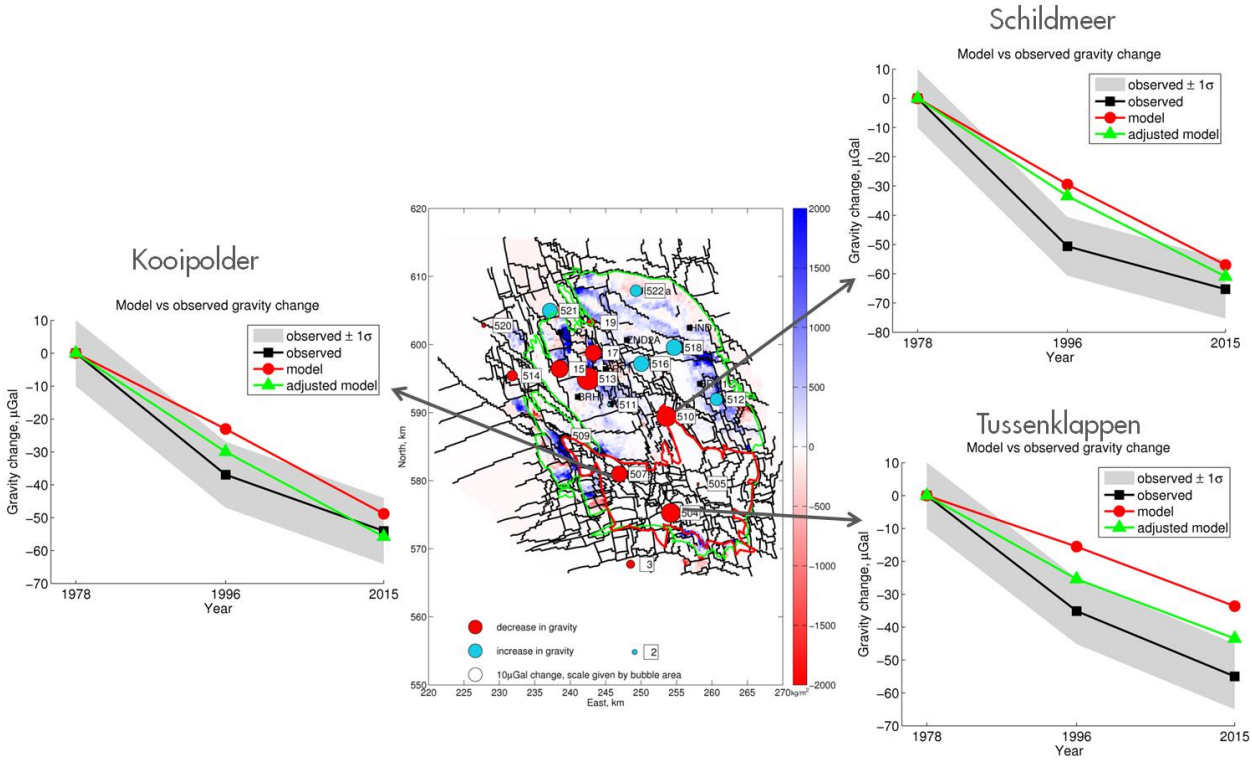

Figure 49: Scenario #2 – Modelled vs observed gravity change (time-series plots, the total signal is shown) for Carboniferous depletion. The middle plot shows 1996-1978 modelled mass change for water (kg/ m², sum over vertical column) with the observed minus modelled gravity difference for the same period.

3.6 Gravity results comparison with other data

The scenario modeling suggests that certain subsurface scenarios will likely yield a good model-to-measurement fit, while honoring additional constraints, such as the PNL data. The sensitivity analysis showed that the mismatches between measured and modeled gravity changes seem to reveal certain patterns. In the North-East of the field, the gravity data support more water influx than what is currently captured in the V2.5 dynamic reservoir simulation model. The simulated water encroachment falls short of the measured encroachment from PNL's. In the South-Western area, where gravity suggests less water influx than modelled, the opposite seems to be true.

The mismatch in the South of the field could be explained by depletion of the Carboniferous. An additional source of information is provided by the subsidence measurements, which are incorporated in the dynamic reservoir model history matching process (Ref. [10]). The mismatch in the subsidence data (Figure 50) seems to align with the gravity change mismatch, i.e. gravity suggests more mass reduction than in the model which is consistent with the model underestimating the measured subsidence.

It is recommended to build the gravity calculations directly into the dynamic reservoir model. This will dismiss the need for stand-alone sensitivity modeling in Matlab (as described in this document) and allow for further refinement of the (assisted) history matching of the dynamic reservoir model by an integrated approach, pursuing a match on gravity data, PNL measurements, and subsidence at the same time.

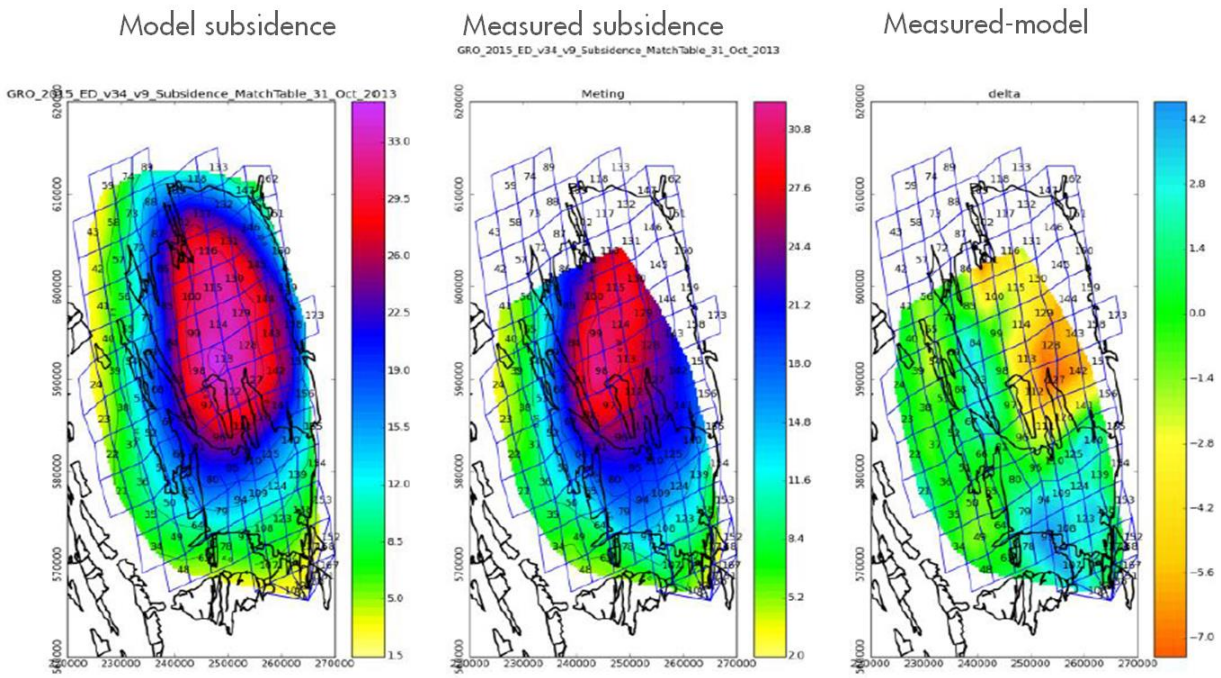

Figure 50: Mismatch between modelled and measured subsidence until 2013. The modeled subsidence is based on Geertsma model (Burkitov et al., 2016)

4 Recommended timing for a repeat survey

Based on the BP2016 production forecast using the 2P reservoir model (Figure 51), predictions were made for the future gravity changes, in order to optimize the timing of a next gravity survey. The results are shown in Figure 52, with all the changes referred to 2015.

The 2015 survey provided excellent data quality with an average station uncertainty of 1.1 μGal. Therefore, when assuming similar data quality for a future survey, there will be a lower time-lapse uncertainty level against the 2015 baseline then against the earlier vintage baselines. Taking into account some additional sources of uncertainty, such as subsidence measurements or groundwater variations, 5 μGal (or better) time-lapse uncertainty can be achieved.

With these assumptions the first detectable gravity changes can be expected in 2021 and the signal will become slightly more robust in 2023. With an increasing time-span, the gravity signal will grow, reaching approximately 10 μGal in 2025 (Table 9). The measured gravity changes might be stronger, considering that no depletion in the Carboniferous was modeled in the BP2016 2P model realization.

With these considerations, it is recommended to acquire a next survey in 2021-2023.

Min/max values in	2019	2021	2023	2025	2027	2031
Total signal (μGal)	-3.9	-5.8	-7.7	-9.7	-11.5	-15.2
Gas (μGal)	-4.3	-6.5	-8.7	-10.9	-13.0	-17.3
Water (μGal)	3.3	4.8	6.3	7.8	9.2	12.1
Gas Production (N.Bcm)	103	152	200	247	294	380

Table 9: Gravity changes with respect to 2015, predicted maximum/minimum values as per BP2016.

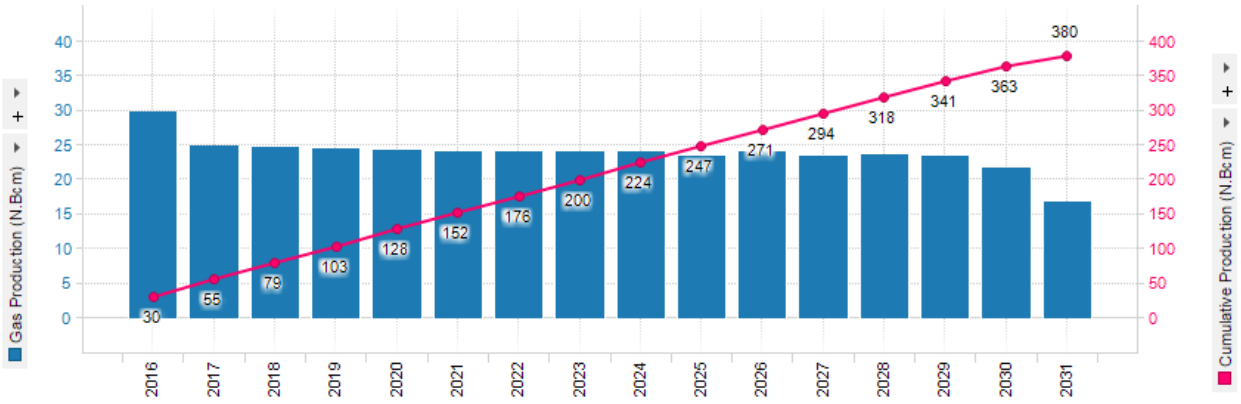

Figure 51: BP2016 production profile

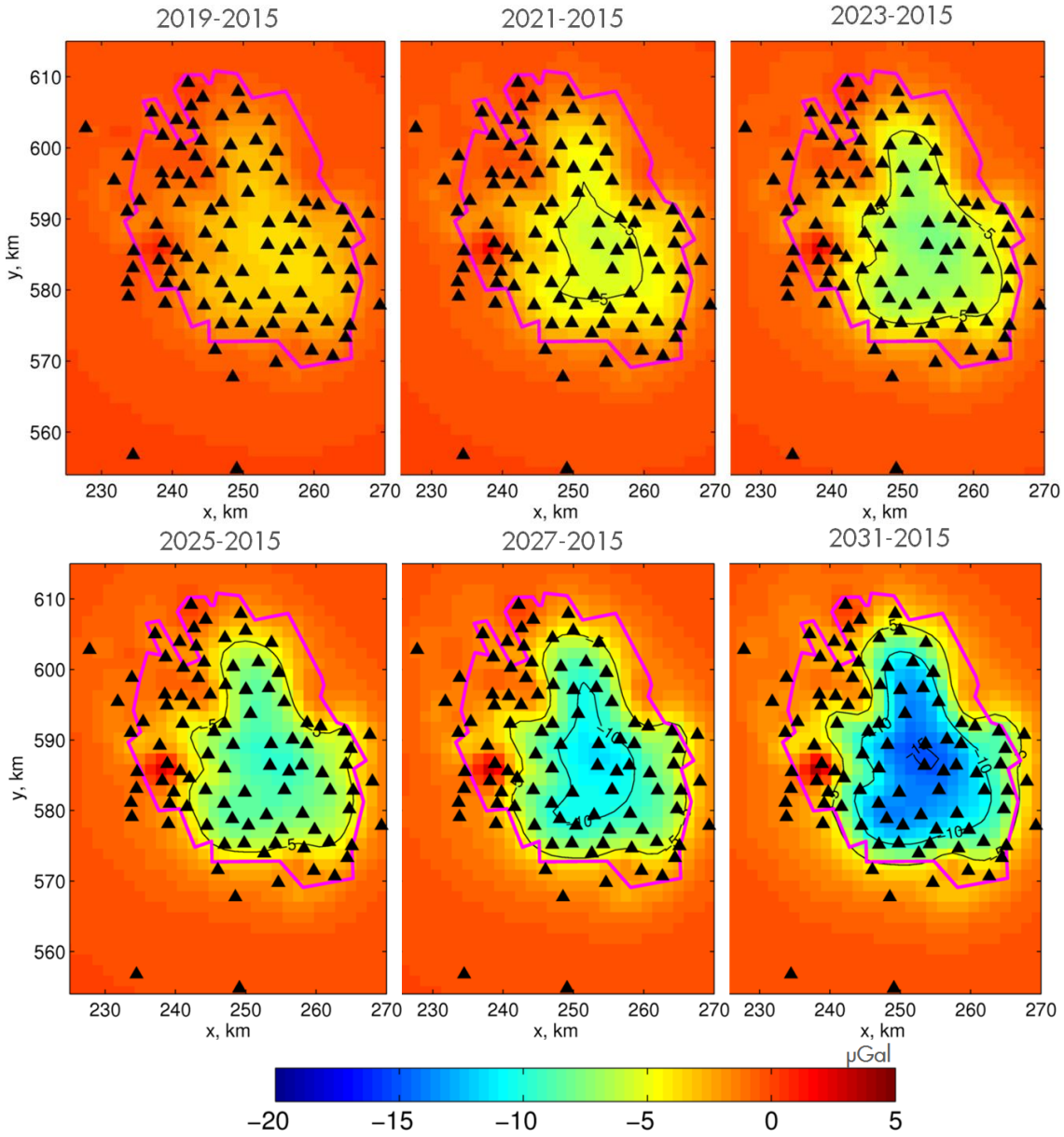

Figure 52: Modeled gravity changes with respect to 2015 based on BP_2016_2P reservoir model predictions. The total gravity change is shown.

5 Conclusions and recommendations:

- The 2015 gravity survey in combination with the reprocessing of historical gravity data resulted in measurable and interpretable gravity changes at a number of stations in the Groningen field.

- Potential influence of groundwater variations on the 1996-1978 and 2015-1978 gravity data interpretation remains limited. The expected gravity noise due to groundwater fluctuations is on average 3-4 μGal and is significantly smaller than measured gravity changes, which are in the order of 50-60 μGal. However, groundwater variations are relevant in the context of future gravity surveys where the measured changes, acquired over shorter time-intervals, are likely to be smaller. Therefore, it is recommended to consider hydrological influences in more detail in the future. This could be achieved by gathering more hydrological data and by measuring groundwater variation in close vicinity of gravity stations. Additional constraints could be provided by regional hydrological models which are being developed by Deltares, constrained and calibrated to in situ hydrological measurements.

- Salt mining in the Groningen area does not add significant noise to the measured 1996-1978 and 2015-1978 gravity changes. The maximum influence is estimated <2 μGal. However, salt extraction noise may be more relevant in the future since a few of the new gravity stations deployed in 2015 are at very close distance from the salt production areas. The signal could reach from a few to several tens of μGal depending on the amount of produced salt. Therefore, it is recommended to gather salt production data and apply necessary corrections in the future.

- Gas production from neighboring fields, like Annerveen, has a very limited impact on measured and future gravity changes at Groningen field.

- Measured gravity changes are consistent with GWC measurements and support more water influx than is currently modelled in the North-East of the field.

- Measured gravity changes are consistent with GWC measurements and support less water influx than is currently modelled in the Stedum area.

- Measured gravity changes support depletion in the gas-bearing part of the Carboniferous. However, this can only partly explain the mismatch between the observed and modeled data. This might be related to the modelling limitations and gravity data uncertainties.

- Based on the BP_2016_2P production forecasts and the associated gravity changes, the acquisition of a next gravity survey is recommended in 2021-2023. The timing needs to be re-evaluated if reservoir production levels change, or if other significant updates to the forecast take place.

- It is recommended to include 1978-1996 gravity changes and 1978-2015 gravity changes at those stations which were not altered significantly into assisted history matching workflow.

- It is recommended to keep track of physical changes at gravity stations by regular inspections at approximately 2 year intervals.

- It is recommended to build the gravity calculations directly into the dynamic reservoir model. This will dismiss the need for stand-alone sensitivity modeling in Matlab and allow for further refinement of the history matching of the dynamic reservoir model by an integrated approach, pursuing a match on reservoir pressure, gravity data, PNL measurements, and subsidence at the same time

6 References

[1] Bilker M. 1996. The relationship between gravity changes and gas extraction in Groningen. MSc thesis, Delft University of Technology.

[2] van Gelderen, M., Haagmans, R. & Bilker, M. 1999. Gravity changes and natural gas extraction in Groningen, Geophysical Prospecting 47(6), 979-993.

[3] van Gelderen, M., Haagmans, R. & Bilker, M. 1998. Natural Gas Extraction and its Induced Gravity Change. DEOS Progress Letter 98.2: 45-56, Delft University of Technology, The Netherlands.

[4] van Hees, S., 1980. Zwaartekrachtmetingen in het Groningen aardsgebied. NGT Geodesia 22 (5), 188-192.

[5] Eiken, O., 2016. Gravimetric monitoring of the Groningen gas field 2015. Data acquisition and processing report.

[6] Vos, L., Lee., D., van der Graaf, A. 2003. Groningen field review: Study of aquifer activity around the Groningen field. ELG-DVC

[7] Pitzer. H. 2015. Groningen gas field monitoring with time-lapse gravity observations. MSc thesis, Delft University of Technology

[8] Paar, W. 2010, Zoutwinning in Nederland, een overzicht. Grondboor&Hamer nr 4/5.

[9] Seubring, J. 1994. Petrophyscial evaluation of the Groningen field Carboniferous. NAM, report number 26649.

[10] Burkitov, U., van Oeveren, H., Valvatne, P. 2016. Groningen Field Review 2015 Subsurface Dynamic Modelling Report. EP201603238100

[11] 5. Nagy, D., Papp, G. & Benedek, J. (2000), 'The gravitational potential and its derivatives for the prism', Journal of Geodesy 74, 552–560.

[12] Abels, J. 22/8/2007. Heiligerlee-1 Pressure Build-Up test (BU) 10/01/07-06/02/07. EP200705213992

Appendix 1. Forward gravity modelling

To model the time-lapse gravity signal, first the temporal mass variations per grid cell are determined using:

$$\Delta m = m_2 - m_1$$
$$= V_p\left[\left(\rho_{g2}S_{g2} + \rho_{w2}S_{w2}\right) - \left(\rho_{g1}S_{g1} + \rho_{w1}S_{w1}\right)\right]$$
$$= V_p\left[\left(\rho_{g2}S_{g2} - \rho_{g1}S_{g1}\right) + \left(\rho_{w2}S_{w2} - \rho_{w1}S_{w1}\right)\right]$$
$$= \Delta m_g + \Delta m_w,$$

with:

$$V_p = NTG \times POR \times GBV$$

whereby:

V_p	pore volume
NTG	Net-to-gross,
POR	porosity,
GBV	grid cell volume,
m	mass,
ρ	density,
S	saturation,

and with the following subscripts:

g	gas
w	water
1	time index for baseline survey (i.e. 1978)
2	time index for repeat survey (e.g., 2015).

The reservoir model outputs are given on a very fine grid consisting of

NX × NY × NZ = 120 × 153 × 43 = 789,480 cells

with approximately lateral dimensions of 350-400m and approximate thickness of 10m.

To compute the gravitational attraction the point mass approximation is applied. In a point mass approximation, the mass change per grid cell is accumulated in a single point aligned with the center of the cell (Figure 53). The point mass gravitational attraction is computed from :

$$\Delta g_k = \gamma \sum_{i=1}^{NX} \sum_{j=1}^{NY} \frac{\Delta m_{ij} z_{ij}}{r_{ij}^3},$$

whereby:

Δg_k modeled time-lapse change in the vertical component of gravity at station k,

γ gravitational constant,

z_{ij} vertical distance between the station k and the center of model cell ij with Δm_{ij}

r_{ij} distance between the station k and the center of model cell ij.

Since the overburden thickness (~2800 m) is significantly larger than the reservoir model cell size the point mass approximation error is negligible and is smaller than 0.5% of the signal (Figure 54).

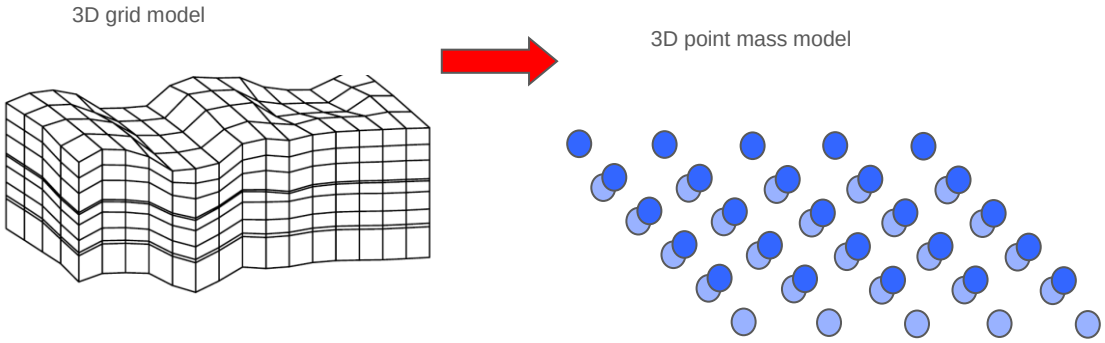

Figure 53: Schematic illustration of a 3D grid model approximation using a set of point masses. The 3D mass redistribution in the reservoir is represented by layers with a number of point masses. One point mass represents the mass variation for a single reservoir cell.

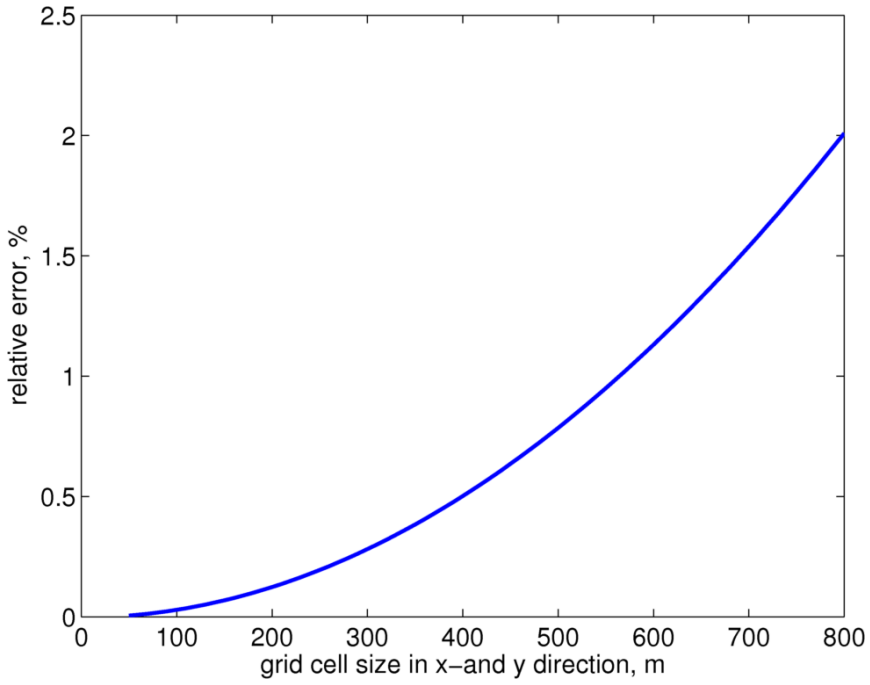

Figure 54: Relative error of point mass gravity approximation vs grid cell size. Results for target depth of 2800 m are shown. The relative error is determined by comparing exact gravity signal calculated for the gridblock geometry (Ref. [11]) with the gravity signal based on point mass approximation.